Tracing deep fluid source contribution to groundwater in an active seismic area (central Italy): A combined geothermometric and isotopic (δ13C) perspective

Tracing deep fluid source contribution to groundwater in an active seismic area (central Italy): A combined geothermometric and isotopic ($\delta^{13}C$) perspective.

M. Barbieri[1], T. Boschetti[2], M. D. Barberio[1], A. Billi[3], S. Franchini[1], Iacumin P.[2], Selmo E.[2] and M. Petitta[1]

[1] Dipartimento di Scienze della Terra, Sapienza University of Rome, Rome, Italy,

[2] Dipartimento di Scienze Chimiche, della Vita e della Sostenibilità Ambientale, University of Parma, Parma, Italy,

[3] Consiglio Nazionale delle Ricerche, IGAG, Rome, Italy

Keywords: active seismic area, geofluids, deep CO_2, $\delta^{13}C(CO_2)$, geothermometry, monitoring

Formattato: Pedice

Formattato: Apice

Formattato: Pedice

Abstract

An understanding of the origin and migration pathways of geofluids in an active seismic area is of paramount importance in terms of societal challenges such as mitigation of seismic hazards. This study investigates the relationship between the stable isotope ratio $^{13}C/^{12}C$ of deep CO_2 and geothermometry in selected groundwater samples located close to extensional faults in central Italy. The temperature range is inferred from an equation based on the Na/Li ratio and chemical geothermal modelling: 113–130°C. Globally, the calculated temperature range agrees with that resulting from deep boreholes in the Northern Apennines. An alternative method is also included to better evaluate the difference in isotopic composition between the aqueous and gaseous $\delta^{13}C(CO_2)$ at deep condition. A review of previously published data shows that monitoring of the isotopic composition of the dissolved inorganic carbon (DIC) in springs of meteoric origin located in seismically active areas must take into account mass and isotopic balance to correctly evaluate the component, and the role, of deep fluid during seismic events. In particular, the coupled (and corrected) isotope and geothermometrical monitoring of the springs could help to distinguish between deep gas or deep fluid contributions to shallow aquifers. The results of this study indicate that faults play a crucial role in controlling the migration of crustal fluids. In addition, they reveal that possible evaluation of potential seismic precursors mandatorily requires a long period of monthly monitoring.

Eliminato: in springs in seismically active areas

1. Introduction

Geofluids have long been known to influence fault-zone motions and related seismic cycles (Smeraglia et al., 2018; Smeraglia et al., 2016; Ünal-İmer et al., 2016; Uysal et al., 2009; Williams et al., 2017); however, little is known about how and where these fluids originate, and how they migrate towards, along, and away from fault zones during the seismic cycle (Person et al., 2007). The increasing importance of these earthquake-related geofluids in the science of seismic precursors (Barberio et al., 2017; De Luca et al., 2018; King et al., 1995; Onda et al., 2018; Skelton et al., 2014; Skelton et al., 2019) makes an understanding of the origin and migration pathways of geofluids of paramount importance in addressing societal challenges such as seismic hazard mitigation.

Fluids with high CO_2 partial pressure are possibly connected with seismic cycles (Skelton et al., 2014; Uysal et al., 2009); therefore, the stable isotope ratio of dissolved inorganic carbon (DIC) has the potential to be a powerful tool for tracing the hydrogeological processes in seismically active areas (Rosen et al., 2018). For instance, deep pressurised fluids, with CO_2 partial pressure of 68–97 MPa and at temperatures between 120–135°C, were tapped through deep boreholes located in the seismically active Umbria–Marche sector of the Apennines, central Italy (also the area of focus of the current study), at depths of 3.70–4.75 km b.s.l. (Collettini et al., 2008). The $\delta^{13}C$(DIC) was used to trace the deep CO_2 in the seismically active area of the Gran Sasso thrust in central Italy (Chiodini et al., 2011), where the relationship between seismic events, hydrothermal anomalies and CO_2-rich deep fluids were also further remarked by Wu et al. (2016). In the surrounding seismogenic sectors, heat anomalies were also inferred in aquifers where CO_2 of endogenic origin dissolves (Chiodini et al., 2013; Di Luccio et al., 2018). Moreover, in some locations of the central Apennines (central Italy) the heat flow could actually be high, but masked by the rapid and abundant shallow circulation of cold groundwater (Duchi et al., 1991; Giustini et al., 2013).

Our main aim in this work is to track the contribution of deep fluid sources to groundwater in seismically active areas of the central Apennines (central Italy). To achieve this, we analyse groundwater samples from

nine selected springs in seismically active areas where upwellings of deep fluids have previously been documented or hypothesised (Figure 1): the Olevano–Antrodoco thrust area (Petitta et al., 2011), the Sulmona plain (Barberio et al., 2017), and the Matese Mountains (Ascione et al., 2014). It should be remarked that, in these areas, no anomalies on stable isotope ratio of oxygen and hydrogen in water molecule, i.e. $\delta^{18}O(H_2O)$ and $\delta^{2}H(H_2O)$, were detected (Barberio et al., 2017; Di Luccio et al., 2018; Petitta et al., 2011; Rosen et al., 2018). In other terms, previous studies showed that all waters could be classified as of meteoric origin, but at the same time the contribution of magmatic/methamorphic fluids (if any) or the isotope fractionations due to water-rock interaction at high temperature seem to be not significant in terms of $\delta^{18}O(H_2O)$ and $\delta^{2}H(H_2O)$ (Clark and Fritz, 1997; McSween et al., 2003; Sheppard, 1986). Differently, the contribution of deep CO_2 gas of magmatic/methamorphic origin to the groundwater of central Italy is well-known and widely documented (Chiodini et al., 2011; Chiodini et al., 2004; Chiodini et al., 2013; Chiodini et al., 2000; Di Luccio et al., 2018; Frondini et al., 2018). However, it is not yet clear whether the contribution of CO_2 occurs only in terms of gas or also by liquid mixing. Therefore, in this study we use and try to combine chemical composition data, the stable isotope ratio $^{13}C/^{12}C$ of the DIC, and sodium-lithium geothermometry to arrive at conclusions regarding how the geofluids originated, and the role of heat anomaly on fluid-mineral thermodynamic equilibria and mixing.

2. Geological and hydrogeological settings

The central Apennines are a late Oligocene-to-present fold-thrust belt generated by the eastward rollback of the Adriatic plate under the European plate (Doglioni, 1991; Malinverno and Ryan, 1986). Specifically, the central Apennine accretionary prism developed through folding and thrusting of the passive continental margin of the Adriatic plate. In central Italy, active contraction is presently located to the east of the belt, below the western Adriatic Sea. The stratigraphic horizons where the basal décollement is located can be recognised from seismic reflection profiles (Bally et al., 1986; Billi et al., 2006; Scrocca, 2006) and are mainly represented by Triassic evaporites located in the lower layers of the passive margin sequence. The sole thrust of the Apennines occurs at more than 20 km in the inner sector (west), shallowing to about 10 km towards the foreland. The thrust sheets are mainly composed of Meso-Cenozoic sedimentary succession, as known

from deep wells drilled in the Apulian-Adriatic foreland. The succession includes, from top to bottom: Meso-Cenozoic limestones and dolostones, Triassic evaporites, and Permian–Triassic phyllites and quartzites. This succession is duplicated and eastward-imbricated in the Apennines fold-thrust belt, where it is also topped by syn- and post-orogenic siliciclastic marine and continental deposits. The Apennines fold-thrust belt is presently cross-cut by Quaternary seismically active normal faults (Cardello and Tesei, 2013; Galli et al., 2002; Galli et al., 2008). In central Italy, two major sub-parallel normal fault systems accommodate the late Pleistocene–Holocene deformation: the eastern and western normal fault systems (Barchi et al., 2000; Boncio et al., 2004; Galadini and Galli, 2001; Roberts and Michetti, 2004) that also controlled the formation of intramountain basins (e.g. L'Aquila, Sulmona, San Vittorino and Fucino basins). Extension is currently active in the axial portion of the central Apennines, where it is responsible for earthquakes of up to M = 7.0 (Barchi et al., 2000; Boschi et al., 1998) and for extension rates of 2.5–3.5 mm/year (Riguzzi et al., 2012). To the west of this area, the Moho is shallow, at 20–25 km (Ponziani et al., 1995), with high heat-flow values of <100 mW m^{-2} (Della Vedova et al., 2001; Mongelli and Zito, 1991) and high levels of CO_2 degassing (Chiodini et al., 2004). More recently, a re-evaluation of the heat flow in the studied area has inferred even higher heat flow of up to 350 mW m^{-2} (Chiodini et al., 2013; Di Luccio et al., 2018).

In the Apennines, both the Cenozoic clayey syn-orogenic deposits and the Triassic anhydritic evaporites are known as important sealing levels for groundwater, hydrocarbons, and deep endogenic gases such as CO_2. Carbon-mass balance calculations, hydrogeochemistry with isotopic and hydrological data, identify the presence of a large flux of deep CO_2 centred in the extended sector of the Apennines, with a large area characterised by a flux greater than 0.45 t d^{-1} km^{-2} (Chiodini et al., 2004; Collettini et al., 2008).

The central Apennines belt is characterised by huge carbonate aquifers with high permeability due to fracturing and karst processes. The Meso-Cenozoic carbonate sequences that host the aquifers are often compartmentalised by layers with low permeability (aquitards and aquicludes), composed of siliciclastic continental/marine deposits (Boni et al., 1986; Petitta et al., 2009). At points of contact with the carbonate aquifers, these deposits act as a permeability boundary, preventing underground hydraulic communication and giving rise to the basal springs of the regional groundwater (Fiorillo et al., 2015).

106 The permeability boundaries between siliciclastic marine and continental deposits and the fractured
107 carbonate aquifers are often represented by normal and thrust faults. Consequently, groundwater frequently
108 undergoes physicochemical changes, which are due to the local upward of mineralising fluids along these
109 tectonic features (Petitta et al., 2011). Groundwater from the carbonate aquifers is subject to these physico-
110 chemical changes upon its movement towards the recent alluvial aquifers. Here, mixing with deep fluids
111 causes groundwater to take on different hydrochemical characteristics. These physicochemical changes may
112 be progressive or fast and localised, depending on the interaction between the tectonic setting and the
113 stratigraphic sequence.

114

115 **3. Methods**

116 *Sampling and analysis*

117 For this study, nine springs were monitored and sampled during the 2018 non-seismic phase. Five springs –
118 Decontra1, Raiano, Bellucci, Le Fonti, Giardino (Table 1) – had been monitored since January 2016, a period
119 matching the hydrogeochemical dataset associated with the 2016–2017 Amatrice–Norcia seismic sequence
120 (central Apennines, Italy) (Barberio et al., 2017). The remaining four springs – Antrodoco, Capovolturno, Rio
121 Freddo and Grassano (Table 1) – were selected because they are directly fed by regional flow in the carbonate
122 aquifers of the central and southern Apennines and they were monitored as potential seismic precursors.

123 At the sampling sites, physicochemical parameters (temperature and pH) were measured using a WTW Multi
124 3420 probe. Carbonate alkalinity was measured by titration using a portable titrator, HCl 0.02N as titrant
125 solution, and bromocresol green as dye indicator (Standard Method 2320 B) (Clesceri et al., 1999). Following
126 filtration in the field (0.45 µm), water aliquots for major and trace cations were acidified at 1% v/v by adding
127 65% p/p HNO_3 Suprapur® (Merck–Millipore). In the laboratory, major ions were analysed with a Chromeleon
128 Dionex (precision ± 2%). An ICS 1100 was used for analysing cations, and a Dionex ICS5000 for analysing
129 anions. According to standard methods (Clesceri et al., 1999), the analytical accuracy levels for major ion
130 ionic balance and for minor trace element determination were better than 5%. Concentrations of minor and

trace elements were measured using an ICPMS (X Series 2, Thermo Fisher Scientific). The total dissolved solids (TDS) in grams per litre was calculated by summing the concentrations of the primary dissolved constituents and half alkalinity as HCO_3^-, i.e.: [0.5 x Alkalinity] + [other dissolved constituents] (Clesceri et al., 1999).

The stable isotope ratio $^{13}C/^{12}C$ of the DIC was determined using water aliquots inferred from previous analyses of the carbonate alkalinity of each specific spring. In the field, the aforementioned water aliquots were injected into 12 ml Na-glass vials (Labco Exetainer®), pre-filled in the laboratory with five droplets of phosphoric acid (ca. 90%) and He gas 6.0 (Spötl, 2005). To limit biological activity and to eliminate the possibility of adding solid particles – especially limestone – to the vials (Dawson, 2017; Li and Liu, 2011), a 0.2 µm polyethersulfone (PES) filter was interposed between the syringe and the needle, with the latter then used to puncture the butyl rubber septa of the vials. In the laboratory, the sample vials were stored in a fridge at 4°C until analysis. A GasBench II (Thermo Fisher Scientific), on-line with a Delta Plus XP mass spectrometer (Thermo Finnigan), was used to determine the 'delta value' of the samples' $\delta^{13}C(DIC)$. These figures were measured and expressed in terms of the 'Vienna–Pee Dee Belemnite (V-PDB)' scale, normalised by assigning the consensus values of -46.6‰ to LSVEC lithium carbonate, +1.95‰ to NBS 19 calcium carbonate (Wieser, 2006), and -5.014‰ to NBS 18. Each sample was analysed in replicate. The accuracy of the method is better than 0.2‰ (2σ).

Thermodynamic and isotopic calculations

The mineral-saturation indexes of the water samples were calculated using PHREEQCI and codes from *The Geochemist's Workbench*, which uses *llnl.dat* and *thermo.dat* thermodynamic datasets coupled with Debye–Hückel and B-Dot theory for the activity, mineral saturation indexes and $CO_2(g)$ partial pressure calculations, respectively (Appelo et al., 2014; Bethke, 2008; Parkhurst and Appelo, 2013). The same codes were also used to calculate the molality (mol/kg H_2O) concentrations of DIC, Ca and SO_4 employed in the following mass balances (Chiodini et al., 2000):

156 $DIC = C_{carb} + C_{ext}$ (1)

157 $C_{carb} = Ca + Mg - SO_4$ (2)

158 $C_{ext} = DIC - C_{carb} = C_{inf} + C_{deep}$ (3)

159 C_{carb} is the amount of carbon derived from the interaction of groundwater with carbonate aquifer rocks, while
160 C_{ext} is carbon derived from processes other than these (i.e. from external sources). This latter component can
161 be expressed as $C_{ext} = C_{inf} + C_{deep}$, where C_{inf} is the carbon from atmospheric and biogenic CO_2, i.e. the
162 infiltrating water. C_{inf} = 2.31E-03 ± 6.1E-04 m has been inferred for the Apennine water recharge (Frondini et
163 al., 2018). C_{deep} is deep CO_2 from metamorphic, mantle, or magma sources (Chiodini et al., 2000).

164 To evaluate the $\delta^{13}C$ isotope composition of deep CO_2 ($\delta^{13}C_{ext}$) in each water sample, the following isotope-
165 mass balance was used (Chiodini et al., 2000):

166 $\delta^{13}C(DIC) \times DIC = (\delta^{13}C_{carb} \times C_{carb}) + (\delta^{13}C_{ext} \times C_{ext})$ (4)

167 The results were compared with those obtained using a subroutine of the NetpathXL code (Parkhurst and
168 Charlton, 2008; Plummer et al., 1994). Using an inorganic carbon-mass and isotope balance similar to those
169 described in equations from (1) to (4), the subroutine, which originated as a tool for radiocarbon dating
170 adjustment (Plummer et al., 1994), calculated the isotope composition of the CO_2(gas) or CO_2(aq) from the
171 $\delta^{13}C$(DIC), taking into account both the complete chemical composition of the water samples and all isotopic
172 fractionation factors between aqueous, mineral (calcite) and gas species (Mook, 1976; Mook, 1980).
173 Moreover, any error in terms of isotope-mass balance due to chemical analysis can be evaluated by using
174 the charge-balancing option (Plummer et al., 1994).

175 In both methods, the value of $\delta^{13}C_{carb}$ = 2.2 ‰ was assumed as the isotopic composition of the carbonate
176 aquifer (Di Luccio et al., 2018; Frondini et al., 2018).

177

178 **4. Results**

According to Schoeller (1962) classification and considering the local average annual air temperature (T_a in Table 1), the temperature of Antrodoco and the three springs from the Sulmona basin fall within in the orthothermal group ($T_a < T < T_a + 4°C$). In contrast, the springs in the southern sector of the studied area are hypothermal ($T < T_a$). However, it should be noted that in the Grassano spring, waters with a mean temperature of 21°C (i.e., thermal T > Ta + 4) were detected (Corniello and De Riso, 1986). All but one of the water samples were fresh (TDS < 1 g/l), with neutral to slightly basic pH (7.07–7.87) and an HCO_3–Ca main chemical composition (Figure 2a). The Figures 2a and 2b also show that the historical chemical composition of the Sulmona springs, in particular Decontra 1 and Raiano, displays chemical variation due to mixing that occurred after the main shocks of earthquakes in 2016–2017 (Boschetti et al., 2019). The exception is the Antrodoco spring sample, which was brackish (TDS = 1.05 g/l), slightly acidic (pH = 6.54), and showed a predominance of calcium on bicarbonate (Ca–HCO_3) and a relatively high sulphate concentration (448 mg/l) in comparison with the HCO_3–Ca springs (from 2.1 mg/l in Rio Freddo to 127 mg/l in Decontra 1). Fluoride and strontium were also higher in the Antrocodo sample (0.9 and 5.2 mg/l, respectively) compared with the other springs (Table 1).

The $\delta^{13}C_{ext}$ results, calculated by Chiodini et al.'s (2000; 2004) method and NetpathXL code (Plummer et al., 1994), are similar when the former is compared with the $\delta^{13}C_{ext}(CO_2)aq$ value obtained by the code (mean difference: ±0.1‰) (Table 2). The slight difference, which falls within the analytical error on isotope measurement of $\delta^{13}C(DIC)$, is mainly due to ion-charge balance correction performed by the code. Moreover, this fact agrees with the assumption in the $\delta^{13}C_{ext}$ calculation that no fractionation occurs during input from any source to the solution (Chiodini et al., 2000). Finally, the $\delta^{13}C_{ext}(CO_2)g$ values are approximately 1‰ more enriched than those for $\delta^{13}C_{ext}(CO_2)aq$ according to the mean $CO_2(g)$-$CO_2(aq)$ fractionation factor at the sampling temperature (Vogel et al., 1970).

5. Discussion

5.1 – $\delta^{13}C_{ext}$ and Na/Li geothermometer

The bicarbonate composition of the investigated water samples is mainly due to interaction with calcites and dolomites of the Mesozoic limestones (Figure 2b). The more peculiar chemical composition of the Antrodoco spring is attributable to a more extensive dissolution of the Triassic sulphate minerals (gypsum-anhydrite of the Burano Formation) (Figure 2b) (Governa et al., 1989; Petitta et al., 2011). This is confirmed by the fact that this sample showed the highest saturation indexes of gypsum-anhydrite (Table 2). The carbon dioxide partial presure calculation showed the highest values in the Antrodoco and Grassano springs: $logPCO_2$(g) of -0.87 and -1.35, respectively. The C_{ext} and the relative $\delta^{13}C_{ext}$ calculations confirm that these samples had the most enriched values (-1.69‰ for Antrodoco and -4.53 ‰ for Grassano), which are within the hypothetical range of the deeply derived CO_2 (from +1‰ to -5‰) (Chiodini et al., 2004; Frondini et al., 2018). At the opposite end of the scale, Giardino, Rio Freddo and Le Fonti springs showed lower $logPCO_2$(g) and a range of $\delta^{13}C_{ext}$ values similar to those typical of the Apennine infiltrating water (Frondini et al., 2018). According to the $\delta^{13}C_{ext}$ versus $1/C_{ext}$ model described by Chiodini et al. (2011), the other springs showed values of carbon contribution between those of the infiltrating water (affected by biogenic carbon) and the deep source (Figure 3a). In detail, the groundwater from Sulmona basin (Raiano, Decontra1 and Bellucci) and Capovolturno fall in the middle of the range. The recalculation of $\delta^{13}C_{ext}$ from the $\delta^{13}C$(DIC) of the Gran Sasso waters (Adinolfi Falcone et al., 2008) shows that the high-altitude snowmelt and groundwater samples plot between typical atmospheric values – $-6.7‰ < \delta^{13}C < -8.2‰$ (Coplen et al., 2002) – and those of the Apennine infiltrating waters, respectively (Figure 3a). An exception is represented by the low-altitude spring of Capopescara, located at the border between the SW Gran Sasso structure and the NE Sulmona basin (Figure 3a) (Adinolfi Falcone et al., 2008). In Chiodini et al. (2013), a heat flow of only 39 MW m^{-2} was inferred for the latter area, in comparison with a higher heat flow value in the northern Gran Sasso structure (176 MW m^{-2}). These data suggest that the $\delta^{13}C_{ext}$ anomalies in the Sulmona basin could be the result of a mixing of fluids from different sources. A relationship between $\delta^{13}C_{ext}$ and the concentration of some dissolved elements suggests a possible contribution, not only of the deep gaseous component, but also of the liquid fraction or a water–mineral re-equilibration due to heat flow. This could be particularly applicable to the samples with the highest $\delta^{13}C_{ext}$ anomalies. In these samples, the correlation between elements (or their ratio) and the CO_2 from the deep source suggests that the application of chemical geothermometers might

be fruitful in terms of inferring the temperature reached by fluids at depth. In the carbonate-evaporite reservoirs of the Apennine, the sodium/lithium Na/Li (Minissale and Duchi, 1988) and sulphate/fluoride SO_4/F (Chiodini et al., 1995; Marini et al., 1986) have been shown to be the most reliable geothermometric equations. In the first case, Minissale and Duchi (1988) applied the Na/Li equation put forward by Fouillac and Michard (1981) to spring waters from the northern Apennines. Application of an updated Na/Li equation by Sanjuan et al. (2014), specifically for the chloride concentration of the waters considered in this study (Cl < 0.3 M), gave temperatures of 96 °C (Antrodoco) and 146 °C (Grassano) (Table 2) and showed a significant correlation with the $\delta^{13}C_{ext}$ (Figure 3b). Indeed, the Pearson's coefficient r is statistically significant ($p < 0.01$) taking into account the number of the samples (N = 8) and the critical value table (df = N – 2, two-tailed test) (Siegle, 2009). Moreover, an ANOVA test on the slope and linearity of the normal probability plot also confirms that the regression is statistically significant (OriginLab, 2017) (Supplementary File S3).

Two water samples from the Sulmona Basin – Decontra 1 and Raiano – showed inferred temperatures of 101°C and 138°C, respectively (Table 2). However, their scattered chemical composition (Figure 2), the $\delta^{13}C_{ext}$ mixed source (Figure 3a) and the local low heat-flow rates suggest that the geothermometric results of the groundwater from Sulmona should be considered prudently. Statistical analysis of 32 samples collected to date at Raiano spring (excluding three outliers – two from before the seismic sequence, and the 06/12/2016 sample, which suffered dilution after the main earthquake shock) shows that the temperatures calculated from the Na/Li ratio were significantly drawn from a normally distributed population (OriginLab, 2017), with $T(Na/Li)_{mean}$ = 126 ± 12°C (1σ) (Supplementary File S4). Lower (similar to local air) or negative temperature values were obtained for the three water samples with $\delta^{13}C_{ext}$ similar to the $\delta^{13}C_{inf}$ of the Apennine infiltrating waters (Giardino, Rio Freddo and Le Fonti springs) (Figure 3b). The application of the SO_4/F equation, specifically for water samples within the low-temperature range (50–150°C; Chiodini et al., 1995), gave negative results for Antrodoco and Grassano and T = 46°C for Rio Freddo. According to Blasco et al. (2018), the unproductive results of the SO_4/F geothermometrical approach could be due to the anhydrite and fluorite undersaturation of the studied waters.

5.2 – Geothermal modelling and recalculation of the $\delta^{13}C_{ext}$

During the upwelling of fluid, its composition could be altered by CO_2 degassing, carbonate precipitation, and mixing with shallow waters. The use of geothermal modelling provides a more reliable approach to reconstructing fluid composition at depth and to estimating reservoir temperature (Battistel et al., 2014). This is mainly because it considers the entire chemical analysis of the involved fluid, rather than just a portion (e.g., elements ratio), thus avoiding some of the restricting assumptions on geothermometric equations based on an elements couple (Bethke, 2008).

In this study, we tried to restore the deep fluid composition of the samples with the highest C_{ext} and $\delta^{13}C_{ext}$ values by recalculating equilibria between water and typical carbonate-evaporite minerals and increasing both temperature and CO_2, thus also attempting to restore the flashed gas. The results obtained from geothermal modelling are close to those determined by the Na/Li geothermometer, with $logPCO_2$ = 1.1 ± 0.3 calculated at the saturated vapour pressure (Figure 4). Finally, the $\delta^{13}C_{ext}$ was recalculated using Netpath code (Plummer et al., 1994) at the mean temperatures obtained by Na/Li and geothermal modelling ($T_{Antrodoco}$ = 113°C; $T_{Grassano}$ = 130°C). Considering the temperatures measured in the Antrodoco 1 borehole (up to 60°C at 3 km) (Trumpy and Manzella, 2017), the temperature inferred for that spring should correspond to a depth of approximatively 5.6 km. The CO_2 partial pressure, alkalinity and the pH were recalculated at the mean temperatures and a total pressure of P = 100 MPa using PHREEQC code and the *phreeqc.dat* thermodynamic dataset, which use the Peng–Robinson equation of state for calculating the solubility of gases at high pressures (Parkhurst and Appelo, 2013). The $\delta^{13}C_{ext}(CO_2)_g$ at the deep temperature and alkalinity values obtained by NetpathXL code were +0.13‰ and -1.28‰ for Antrodoco and Grassano, respectively (Table 3). These latter values are enriched at +0.8‰ and +2.3‰ compared to the $\delta^{13}C_{ext}(CO_2)_g$ values obtained by the same code at sampling conditions. In the Burano formation at Antrodoco, the followings values for carbonate minerals were detected: $\delta^{13}C_{dolomite}$ = +2.7‰ and $\delta^{13}C_{calcite}$ = +1.6‰ (Masi et al., 1995). The central value between the two carbonates is close to the mean value employed for limestones in central Italy used for the $\delta^{13}C_{ext}$ calculation (i.e., $\delta^{13}C_{carb}$ = +2.2‰) (Di Luccio et al., 2018; Frondini et al., 2018). NetpathXL code permits a differentiation of the isotope composition of both calcite and dolomite in order to obtain a more accurate

283 evaluation of the deep $\delta^{13}C(CO_2)$. The obtained $\delta^{13}C_{ext}(CO_2)_g$ = +0.095‰ for Antrodoco is slightly higher than
284 the aforementioned value, i.e. $\delta^{13}C_{ext}(CO_2)_g$ = +0.13‰. However, this difference is negligible in the light of
285 the accuracy of the $\delta^{13}C$(DIC) analytical method. A similar approach has been employed to infer deep
286 $\delta^{13}C_{ext}(CO_2)_g$ values at Raiano. The geochemical modelling applied to that sample produced a temperature of
287 T = 129°C (Supplementary File S4), which is within the historical mean obtained by the Na/Li geothermometer
288 (T = 126 ± 12°C; Supplementary File S5). At that temperature, the carbon dioxide partial pressure at the
289 saturated vapour pressure is $logPCO_2(g)$ = 0.82, whereas it is approximately 1.3 at the total pressure of 100
290 MPa (Table 3). The mean temperature of T = 127°C for that spring could be compatible with a fluid from a
291 depth of approximately 7 km that is within a complex thrust zone where late Triassic evaporites (Anidriti di
292 Burano formation) are tectonically interbedded with late Permian–Triassic quartzites and phyllites
293 (Verrucano formation) (Romano et al., 2013; Santilano et al., 2019). The recalculated $\delta^{13}C_{ext}(CO_2)_g$ = -3.36‰
294 is significantly different from the value at sampling condition; i.e. $\delta^{13}C_{ext}(CO_2)_g$ = -6.67‰ (Table 2). However,
295 the values inferred for Antrodoco and Grassano are closer to the $\delta^{13}C_{ext}$ values of 0‰ and -1.5‰, as recently
296 calculated for the deep source end-member in the central Apennine area (Chiodini et al., 2013; Di Luccio et
297 al., 2018).

298 *5.3 – Waters sampled during the 2016–2017 central Italy seismic sequence*

299 After testing the above-described method with chemical and isotopic $\delta^{13}C$(DIC) data from our dataset
300 referring to the non-seismic sequence (2018, see Table 1), we also applied the same method to the chemical
301 and isotopic data collected by Rosen et al. (2018) during the seismic sequence in Amatrice–Norcia during
302 2016–2017 in order to evaluate possible geochemical anomalies related to the seismic cycle.

303 The chemical and isotope compositions of four springs were studied during the seismic sequence that
304 occurred in central Italy between August 2016 and January 2017 (Rosen et al., 2018). In that study, the
305 authors reported that the postmainshock $\delta^{13}C$(DIC) value range of the waters was from -5‰ to -3‰, placing
306 it within the range of mantle-derived CO_2 in the central Apennines; i.e. -5‰ to -1‰ (Chiodini et al., 2004;
307 Chiodini et al., 2000). However, they did not perform the necessary isotope-mass balance to determine the
308 $\delta^{13}C_{ext}$. Indeed, even higher $\delta^{13}C$(DIC) values (up to +2.2‰) were measured in the PES springs during periods

of non-seismic alarm (Civita and Fiorucci, 2010). In Figure 5, we plotted the recalculated $\delta^{13}C_{ext}$ and C_{ext} parameters from the chemical and isotope values published by Rosen et al. (2018) (Supplementary File S6). In that manuscript, the most enriched $\delta^{13}C$(DIC) values were detected in PES and SUS springs. In terms of the recalculated $\delta^{13}C_{ext}$, these samples are clustered between the 'deep' and 'C_{inf}' sources (Figure 5a), which are similar to the so-called 'group B' water samples of Chiodini et al. (2011). However, despite the addition of deeply derived CO_2, the highest $\delta^{13}C_{ext}$ detected in a PES spring on 31 October 2016 (i.e. one day after the main shock on 30 October 2016) was not higher than -6‰. It should be also noted that during the seismic sequence the PES spring samples also showed a linear path when $\delta^{13}C_{ext}$ is plotted against the temperatures inferred by the Na/Li geothermometer (Figure 5b). This fact testifies to the addition of a liquid deep source, which is characteristic of the St. Vittorino plain (Petitta et al., 2011). Indeed, deep fluid with a lithium concertation up to 200 μg/l has been measured in that area (Cotilia's Spa) (Civita and Fiorucci, 2010). This also agree with the abrupt changes at PES spring of the calculated Na/Li temperature and $\delta^{13}C_{ext}$ during the seismic sequences of the 2016-2017 (Figure 6a). In contrast, SUS samples depicted $\delta^{13}C_{ext}$ variation at an almost constant Na/Li ratio, probably due to an ingression of only the gas phase (and no liquid) from the deep source. However, the mixing between deep and shallow sources at PES springs is supposed to be quite normal, presumably constant, but with variable proportions. This hypothesis is supported by the historical concentration data regarding sodium and lithium detected in that spring (Barbieri et al., 2017; Civita and Fiorucci, 2010) (Figure 6b), which confirm that mixing also occurred during periods without earthquake warnings. Rather, the anomalous Na/Li ratio detected on 31 October 2016 (Figure 5b) could be due to: i) an increased contribution from the shallow source after a post-seismic permeability change (Charmoille et al., 2005); ii) a change of mineralisation potentially affecting the character of a fault slip in response to earthquakes (Bense et al., 2013); or iii) a combination of both of these phenomena.

6. Conclusions

The chemical composition and stable isotope ratio $^{13}C/^{12}C$ of the DIC of nine selected springs from the central Apennines show a correlation between the temperatures inferred by geothermometers and the isotopic

composition of the deep CO_2 gas of magmatic/methamorphic origin (the so-called C_{ext}), which is dissolved in water as $CO_2(aq)$. In particular, the sodium–lithium geothermometric equation allows direct verification of this correlation. Among the studied spring-water samples, those from the Olevano–Antrodoco and the Matese fault systems showed the most promising results for studying deep fluids. In the Sulmona basin, the Raiano spring showed the most enriched values in term of $\delta^{13}C_{ext}$ and the related deep temperature. The inferred range of temperature (113–130°C) and the mean CO_2 partial pressure calculated at depth ($logPCO_2$ = 1.1 ± 0.3) for these three springs are comparable with figures obtained from deep boreholes in the northern Apennines (Collettini et al., 2008). The observed correlation between $\delta^{13}C_{ext}$ and Na/Li temperature was also verified in samples collected during a seismic sequence and recalculated from Rosen et al. (2018). Therefore, in terms of the endogenic CO_2 flow and the seismic cycle of the study area, we can infer from our results that the monthly samples performed in our study are useful for distinguishing between springs which receive deep CO_2 contributions only and those having a mix of gas plus liquid phases. The combined results of $\delta^{13}C_{ext}$ and Na/Li ratio data demonstrate that mixing between deep and shallow fluids occurs in seismic area of central Italy. The former acquires CO_2 gas of endogenic source and equilibrated with aquifer minerals at temperature not higher than 150 °C. Differently to high temperature seismic area as Iceland or Japan (bibliografia), the temperature range detected in the studied groundwater is not higher enough to produce a ^{18}O-enrichment in the water molecule due to interaction with minerals (e.g. Giggenbach, 1992). This could explain the reason why no significant $\delta^{18}O(H_2O)$ variations were detected during seismic swarms (Barberio et al., 2017; Rosen et al., 2018). Shallow groundwater are characterized by a biogenic signature of the dissolved carbon dioxide, which is typical of infiltrating waters (the so-called C_{inf}), and Na/Li ratio correspondig to a low temperature water-mineral equilibria. However, data showed that they could mix with deep fluid consequently to a post-seismic permeability change. However, the combined and complex response of Na/Li and C_{ext} variations during an earthquake sequence necessarily requires an historical chemical and isotope dataset to allow for a complete and in-depth understanding of the complex hydrogeological and geochemical processes involved, with the ultimate aim of evaluating the possible hydrogeochemical precursors of earthquakes.

Acknowledgements: This work was partially funded by Fondazione ANIA (www.fondazioneania.it) through the HydroQuakes Project involving Fondazione ANIA, Istituto di Geologia Ambientale e Geoingegneria (IGAG-CNR), and Sapienza Università di Roma. We thank Dr Umberto Guidoni (Fondazione ANIA) and his collaborators for granting the permit to publish these results.

Tables and Figures Captions

Table 1 – Physicochemical composition and stable isotope ratio of dissolved inorganic carbon $\delta^{13}C(DIC)$ of the sampled waters. Minor and trace elements (µg/l) are detailed in the Supplementary File S1.

Table 2 – Na/Li geothermometer results (Sanjuan et al., 2014); concentration (molality) and isotope composition of carbon from the deep source, C_{ext} and $\delta^{13}C_{ext}$ respectively; saturation indexes and carbon dioxide partial pressure from thermodynamic calculation (detailed results and precision measures are presented in the Supplementary File S2).

Table 3 – Recalculation of some parameters, at depth conditions, for the three samples that showed the most enriched $\delta^{13}C_{ext}$ (Table 2). The physico-chemical conditions at P = 100 MPa were recalculated using PHREEQC code and phreeqc.dat, which use the Peng–Robinson equation of state for calculating the solubility of gases at high pressure (Parkhurst and Appelo, 2013). Mean temperature derived from Na/Li equation at Cl < 0.3M (Sanjuan et al., 2014) and geothermal modelling. $\delta^{13}C_{ext}(CO_2)_g$ derived from NetpathXL code (Plummer et al., 1994), assuming $\delta^{13}C_{carb}$ = +2.2‰ for both calcite and dolomite (Di Luccio et al., 2018; Frondini et al., 2018).

Figure 1 – Map of central Apennines (see location in upper left inset). Seismic data (including focal mechanisms) are from the INGV database (available online at http://cnt.rm.ingv.it/) between January 1st, 2000, and June 15th, 2019 (Mw ≥ 3.5).Historical earthquakes (M_w>6.5) are from INGV historical catalogue (available online at http://www.mi.ingv.it/terremoti-storici/). Base digital elevation model is from the ISPRA database SINAnet (available online at http://www.sinanet.isprambiente.it/it). Location of the monitoring springs analyzed in this work are displayed by blue drops while those analyzed in other works are displayed by white ones. Faults (red and orange lines, normal and thrust faults respectively) are from the Ithaca database (available online at http://www.isprambiente.gov.it/en/projects/soil-and-territory/italy-hazards-from-capable-faulting).

Figure 2 – Langelier–Ludwig (a) and calcium versus bicarbonate concentration (b) diagrams of the waters sampled in this study (black squares with white codes) compared with data from existing literature: coloured symbols are from the Sulmona basin (Barberio et al., 2017), light grey from the Antrodoco area (Petitta et al., 2011), and dark grey from the Grassano area (Corniello and De Riso, 1986). In both diagrams: dissolved constituents concentrations in equivalent.

Figure 3 – a) $\delta^{13}C_{ext}$ versus $1/C_{ext}$ diagram. C_{inf} area: $\delta^{13}C_{ext}$ = -21.6 ± 2.9 ‰ ‰ and C_{ext} = 2.31 ± 0.61 mmol (Frondini et al., 2018); deep source: $\delta^{13}C_{ext}$ from -5 ‰ to +1 ‰ and $1/C_{ext}$ = 0 (Chiodini et al., 2004; Frondini et al., 2018). b) $\delta^{13}C_{ext}$ versus 1/T, where T = temperature in °C obtained from Na/Li geothermometer (Sanjuan et al., 2014), versus $\delta^{13}C_{ext}$. The Pearson's coefficient r is statistically significant ($p < 0.01$) taking into account the number of the samples (N = 8) and the critical value table (df = N – 2, two-tailed test) (Siegle, 2009). In both diagrams, black squares with white codes are water samples from this study. In a): crosses depict groundwater and snowmelt samples from Gran Sasso massif (Adinolfi Falcone et al., 2008); 'Degassing water' field depicts enriched $\delta^{13}C_{ext}$ value, e.g. in Cotilia springs (Chiodini et al., 2011; Giustini et al., 2013; Petitta et al., 2011); light grey squares represent Raiano spring (Sulmona basin) samples from 14/04/2009 to 19/02/2010 (Chiodini et al., 2011), whereas dark grey circles and square the respectively bicarbonatic and sulphatic waters sampled at Antrodoco (Petitta et al., 2011).

Spostato (inserimento) [1]

Codice campo modificato

Spostato in su [1]: 'Degassing water' field depicts enriched $\delta^{13}C_{ext}$ value, e.g. in Cotilia springs (Chiodini et al., 2011; Giustini et al., 2013; Petitta et al., 2011).

Eliminato: .

Figure 4 – Antrodoco and Grassano geothermal modelling calculated using the React tool of *The Geochemist's Workbench* (Bethke, 2008) and thermo.dat thermodynamic dataset. Red lines and blue lines depict the variation mineral saturation indexes and partial pressure of carbon dioxide at increasing temperature, respectively.

Figure 5 – Recalculated $\delta^{13}C_{ext}$ (‰ vs. V-PDB), C_{ext} (mol) and Na/Li geothermometrical temperature (°C) parameters of the NER, PES, SUS and VIC springs collected during the 2016–2017 central Italy seismic sequence (Rosen et al., 2018) (Supplementary File S6). In a): $\delta^{13}C_{ext}$ versus $1/C_{ext}$ diagram (fields as in Figure 3); in b): $\delta^{13}C_{ext}$ versus 1/T, where T = temperature in °C obtained from Na/Li geothermometer (Sanjuan et al., 2014). In b), the solid line depicts the linear best-fit shown in Figure 3b, along with its confidence (dotted-dashed curves) and prediction (dotted curves) intervals, calculated at 95% confidence level (OriginLab, 2017). The error bar depicts the variations of the two parameters in the NER waters.

Figure 6 – a) Time series for Na/Li geothermometrical temperature (°C) and $\delta^{13}C_{ext}$ (‰ vs. V-PDB) during the 2016-2017 central Italy seismic sequence as recalculated from chemical and isotope of Rosen et al. (2018); vertical arrows depict the main seismic events: ①: 08/24/2016, ②: from 10/26/2016 to 10/30/2016, ③: 01/18/2017. b) Historical sodium versus lithium concentration (mol/l) of the PES spring (Peschiera–Velino river valley, central Italy) (Barbieri et al., 2017; Civita and Fiorucci, 2010; Rosen et al., 2018). The variation in the concentration of the two elements at 'deep source' (Barbieri et al., 2017; Civita and Fiorucci, 2010; Tassi et al., 2012) and 'shallow water' (Barbieri et al., 2017) are depicted by error bars. These two components represent the main end-members (along with meteoric recharge, approximately at the origin of the axes) involved in the mixing that produces the PES-spring variation (Barbieri et al., 2017; Civita and Fiorucci, 2010).

Supplementary File S1 – Concentration of minor and trace elements, in µg/l, determined by ICP-MS.

Supplementary File S2 – Minerals saturation indexes and CO_2 partial pressure as $logPCO_2$.

Supplementary File S3 – Statistics of Na/Li geothermometer results vs. $\delta^{13}C_{ext}$ linear regression (Figure 3b).

Codice campo modificato

Formattato: Inglese (Stati Uniti)

Formattato: Inglese (Stati Uniti)

Supplementary File S4 – Descriptive statistics and normality test (OriginLab, 2017) of the temperature results obtained by Na/Li geothermometrical equation at Cl < 0.3M (Sanjuan et al., 2014) and applied to historical and unedited data measured at Raiano spring (Sulmona basin).

Supplementary File S5 - Geothermal modelling of Raiano spring calculated using the React tool of *The Geochemist's Workbench* (Bethke, 2008) and thermo.dat thermodynamic dataset.

Supplementary File S6 - Recalculated $\delta^{13}C_{ext}$ (‰ vs. V-PDB), C_{ext} (mol) and Na/Li geothermometrical temperature (°C) (Sanjuan et al., 2014) parameters of the NER, PES, SUS and VIC springs collected during the 2016–2017 central Italy seismic sequence (Rosen et al., 2018).

References

Adinolfi Falcone, R., Falgiani, A., Parisse, B., Petitta, M., Spizzico, M., Tallini, M., 2008. Chemical and isotopic ($\delta^{18}O$‰, $\delta^{2}H$‰, $\delta^{13}C$‰, ^{222}Rn) multi-tracing for groundwater conceptual model of carbonate aquifer (Gran Sasso INFN underground laboratory–central Italy). Journal of Hydrology, 357: 368-388. DOI:10.1016/j.jhydrol.2008.05.016

Appelo, C.A.J., Parkhurst, D.L., Post, V.E.A., 2014. Equations for calculating hydrogeochemical reactions of minerals and gases such as CO_2 at high pressures and temperatures Geochimica et Cosmochimica Acta, 125: 49-67. DOI:https://doi.org/10.1016/j.gca.2013.10.003

Ascione, A., Bigi, S., Ciotoli, G., Corradetti, A., Etiope, G., Ruggiero, L., Sacco, P., Tartarello, C., Tavani, S., Valente, E., 2014. The southern Matese active fault system: New geochemical and geomorphological evidence. In: Eva, E., Galli, P. (Eds.), Atti 33 Convegno Nazionale GNGTS, Tema 1: Geodinamica, Bologna, pp. 11-19.

Bally, A.W., Burbi, L., Cooper, C., Ghelardoni, R., 1986. Balanced sections and seismic reflection profiles across the central Apennines. Memorie della Società Geologica Italiana, 35: 257–310.

Barberio, M.D., Barbieri, M., Billi, A., Doglioni, C., Petitta, M., 2017. Hydrogeochemical changes before and during the 2016 Amatrice-Norcia seismic sequence (central Italy). Scientific Reports, 71(1). DOI:10.1038/s41598-017-11990-8

Barbieri, M., Nigro, A., Petitta, M., 2017. Groundwater mixing in the discharge area of San Vittorino Plain (Central Italy): geochemical characterization and implicationfor drinking uses. Environmental Earth Sciences, 76(393). DOI:https://doi.org/10.1007/s12665-017-6719-1

Barchi, M., Galadini, F., Lavecchia, G., Messina, P., Michetti, M., Peruzza, L., Pizzi, A., Tondi, E., Vittori, E., 2000. Sintesi delle conoscenze sulle faglie attive in Italia centrale: parametrizzazione ai fini della caratterizzazione della pericolosità sismica, GNDT-Monografie. Report for CNR — Gruppo Nazionale per la Difesa dai Terremoti (GNDT).

Formattato: Italiano (Italia)
Codice campo modificato
Formattato: Italiano (Italia)
Codice campo modificato
Formattato: Italiano (Italia)
Formattato: Italiano (Italia)
Formattato: Italiano (Italia)
Formattato: Italiano (Italia)
Codice campo modificato

Battistel, M., Hurwitz, S., Evans, W., Barbieri, M., 2014. Multicomponent geothermometry applied to a medium-low enthalpy carbonate-evaporite geothermal reservoir. Energy Procedia, 59: 359-365. DOI:https://doi.org/10.1016/j.egypro.2014.10.389

Bense, V.F., Gleeson, T., Loveless, S.E., Bour, O., Scibek, J., 2013. Fault zone hydrogeology. Earth-Science Reviews, 127: 171-192. DOI:http://dx.doi.org/10.1016/j.earscirev.2013.09.008

Bethke, C.M., 2008. Geochemical and biogeochemical reaction modeling. Cambridge University Press, New York.

Billi, A., Tiberti, M.M., Cavinato, G.P., Cosentino, D., Di Luzio, E., Keller, J.V.A., Kluth, C., Orlando, L., Parotto, M., Praturlon, A., Romanelli, M., Storti, F., Wardell, N., 2006. First results from the CROP-11 deep seismic profile, central Apennines, Italy: evidence of midcrustal folding. Journal of the Geological Society of London, 163: 583–586. DOI:https://doi.org/10.1144/0016-764920-002

Blasco, M., Gimeno, M.J., Auqué, L.F., 2018. Low temperature geothermal systems in carbonate-evaporitic rocks: Mineral equilibria assumptions and geothermometrical calculations. Insights from the Arnedillo thermal waters (Spain). Science of the Total Environment, 615: 526-539. DOI:https://doi.org/10.1016/j.scitotenv.2017.09.269

Boncio, P., Lavecchia, G., Pace, B., 2004. Defining a model of 3D seismogenic sources for Seismic Hazard Assessment applications: the case of central Apennines (Italy). Journal of Seismology, 8(3): 407–425. DOI:https://doi.org/10.1023/B:JOSE.0000038449.78801.05

Boni, C.F., Bono, P., Capelli, G., 1986. Schema Idrogeologico dell'Italia Centrale – A) Carta idrogeologica (scala 1:500.000); B) Carta idrologica (scala 1:500.000); C) Carta dei bilanci idrogeologici e delle risorse idriche sotterranee (scala 1:1.000.000) Memorie della Società Geologica Italiana, 35(2): 991-1012.

Boschetti, T., Barbieri, M., Barberio, M.D., Billi, A., Franchini, S., Petitta, M., 2019. CO_2 Inflow and Elements Desorption prior to a Seismic Sequence, Amatrice-Norcia 2016, Italy. Geochemistry, Geophysics, Geosystems, 20. DOI:https://doi.org/10.1029/2018GC008117

Boschi, E., Guidoboni, E., Ferrari, G., Valensise, G., 1998. I terremoti dell'Appennino Umbro-Marchigiano: area sud orientale dal 99 a.C. al 1984. Istituto Nazionale di Geofisica; SGA - Compositori, Bologna.

Cardello, G.L., Tesei, T., 2013. Transtensive faulting in carbonates at different crustal levels: examples from SW Helvetics and Central Apennines. Rendiconti Online della Società Geologica Italiana, 29: 20–23.

Charmoille, A., Fabbri, O., Mudry, J., Guglielmi, Y., Bertrand, C., 2005. Post-seismic permeability change in a shallow fractured aquifer following a ML 5.1 earthquake (Fourbanne karst aquifer, Jura outermost thrust unit, eastern France). Geophysical Research Letters, 32(18). DOI:https://doi.org/10.1029/2005GL023859

Chiodini, G., Caliro, S., Cardellini, C., Frondini, F., Inguaggiato, S., Matteucci, F., 2011. Geochemical evidence for and characterization of CO_2 rich gas sources in the epicentral area of the Abruzzo 2009 earthquakes. Earth and Planetary Science Letters, 304(3-4): 389-398.

Chiodini, G., Cardellini, C., Amato, A., Boschi, E., Caliro, S., Frondini, F., Ventura, G., 2004. Carbon dioxide Earth degassing and seimogenesis in central and southern Italy. Geophysical Research Letters, 31(7). DOI:http://dx.doi.org/10.1029/2004GL019480

Chiodini, G., Cardellini, C., Caliro, S., Chiarabba, C., Frondini, F., 2013. Advective heat transport associated with regional Earth degassing in central Apennine (Italy). Earth and Planetary Science Letters, 373: 65-74. DOI:http://dx.doi.org/10.1016/j.epsl.2013.04.009

Formattato: Italiano (Italia)

Formattato: Italiano (Italia)

Codice campo modificato

Codice campo modificato

Formattato: Italiano (Italia)

Formattato: Italiano (Italia)

Formattato: Italiano (Italia)

Formattato: Italiano (Italia)

Codice campo modificato

513 Chiodini, G., Frondini, F., Cardellini, C., Parello, F., Peruzzi, L., 2000. Rate of diffuse carbon dioxide Earth
514 degassing estimated from carbon balance of regional aquifers: the case of central Apennine, Italy.
515 Journal of Geophysical Research: Solid Earth, 105(B4): 8423-8434.
516 DOI:https://doi.org/10.1029/1999JB900355

517 Chiodini, G., Frondini, F., Marini, L., 1995. Theoretical geothermometers and PCO_2 indicators for aqueous
518 solutions coming from hydrothermal systems of medium-low temperature hosted in carbonate-
519 evaporite rocks. Application to the thermal springs of the Etruscan Swell, Italy. Applied
520 Geochemistry, 10(3): 337-346.

521 Civita, M.V., Fiorucci, A., 2010. The recharge - discharge process of the Peschiera spring system (central Italy).
522 AQUA mundi, Am02019(2): 161-178. DOI:10.4409/Am-014-10-0019

523 Clark, I.D., Fritz, P., 1997. Environmental Isotopes in Hydrogeology. CRC Press.

524 Clesceri, L.S., Greenberg, A.E., Eaton, A.D., 1999. Method 1030 E. Checking Correctness of Analyses, Standard
525 methods for the examination of water and wastewater. American Public Health Association,
526 American Water Works Association, Water Environment Federation, Washington.

527 Collettini, C., Cardellini, C., Chiodini, G., De Paola, N., Holdsworth, R.E., Smith, S.A.F., 2008. Fault weakening
528 due to CO_2 degassing in the Northern Apennines: short-and long-term processes. . In: Wibberley,
529 C.A.J., Kurz, W., Imber, J., Holdsworth, R.E., Collettini, C. (Eds.), The Internal Structure of Fault Zones:
530 Implications for Mechanical and Fluid-Flow Properties. Geological Society, London, Special
531 Publications. The Geological Society of London, London, pp. 175-194. DOI:10.1144/SP299.11

532 Coplen, T.B., Hopple, J.A., Böhlke, J.K., Peiser, H.S., Rieder, S.E., Krouse, H.R., Rosman, K.J.R., Ding, T., Vocke,
533 R.D., Révész, K.M.J., Lamberty, A., Taylor, P., De Bièvre, P., 2002. Compilation of minimum and
534 maximum isotope ratios of selected elements in naturally occurring terrestrial materials and
535 reagents, U.S. Department of the Interior, U.S. Geological Survey, Reston, Virginia.

536 Corniello, A., De Riso, R., 1986. Idrogeologia e idrochimica delle sorgenti dell'Agro Telesino (BN). Geologia
537 Applicata e Idrogeologia, 21: 53-84.

538 Dawson, K., 2017. Gasbench II analysis of dissolved inorganic carbon (DIC),
539 https://www.protocols.io/view/gasbench-ii-analysis-of-dissolved-inorganic-carbon-g5pby5n.
540 DOI:dx.doi.org/10.17504/protocols.io.g5pby5n

541 De Luca, G., Di Carlo, G., Tallini, M., 2018. A record of changes in the Gran Sasso groundwater before, during
542 and after the 2016 Amatrice earthquake, central Italy. Scientific Report, 8.
543 DOI:https://doi.org/10.1038/s41598-018-34444-1

544 Della Vedova, B., Bellani, S., Pellis, G., Squarci, P., 2001. Deep temperatures and surface heat flow
545 distribution. In: Vai, G.B., Martini, P. (Eds.), Anatomy of an Orogen, The Apennines and Adjacent
546 Mediterranean Basins. Kluwer Academic Publishers, Dordrecht, pp. 65–76.
547 DOI:https://doi.org/10.1007/978-94-015-9829-3_7

548 Di Luccio, F., Chiodini, G., Caliro, S., Cardellini, C., Convertito, V., Pino, N.A., Tolomei, C., Ventura, G., 2018.
549 Seismic signature of active intrusions in mountain chains. Science Advances, 4(1).
550 DOI:10.1126/sciadv.1701825

551 Doglioni, C., 1991. A proposal of kinematic modelling for W-dipping subductions - possible applications to
552 the Tyrrhenian - Apennines system. Terra Nova, 3(4): 423-434. DOI:10.1111/j.1365-
553 3121.1991.tb00172.x

Formattato: Italiano (Italia)
Formattato: Italiano (Italia)
Codice campo modificato
Codice campo modificato
Formattato: Italiano (Italia)
Formattato: Italiano (Italia)
Formattato: Italiano (Italia)
Formattato: Italiano (Italia)
Codice campo modificato

Duchi, V., Paolieri, M., Pizzetti, A., 1991. Geochemical study on natural gas and water discharges in the Southern Latium (Italy): circulation, evolution of fluids and geothermal potential in the region. Journal of Volcanology and Geothermal Research, 47(3-4): 221-235. DOI:https://doi.org/10.1016/0377-0273(91)90002-H

Fiorillo, F., Pagnozzi, M., Ventafridda, G., 2015. A model to simulate recharge processes of karst massifs: a model to simulate recharge processes of karst massifs. Hydrological Processes, 29: 2301–2314. DOI:https://doi.org/10.1002/hyp.10353

Fouillac, C., Michard, G., 1981. Sodium/lithium ratio in water applied to geothermometry of geothermal reservoirs. Geothermics, 10(1): 55-70. DOI:https://doi.org/10.1016/0375-6505(81)90025-0

Frondini, F., Cardellini, C., Caliro, S., Beddini, G., Rosiello, A., Chiodini, G., 2018. Measuring and interpreting CO_2 fluxes at regional scale: the case of the Apennines, Italy. Journal of the Geological Society. DOI:https://doi.org/10.1144/jgs2017-169

Galadini, F., Galli, P., 2001. Archaeoseismology in italy: case studies and implications on long-term seismicity. Journal of Earthquake Engineering, 5(1): 35–68. DOI:https://doi.org/10.1080/13632460109350385

Galli, P., Galadini, F., Moro, M., Giraudi, C., 2002. New paleoseismological data from the Gran Sasso d'Italia area (central Apennines). Geophysical Research Letters, 29(2): 38–41. DOI:https://doi.org/10.1029/2001GL013292

Galli, P., Galadini, F., Pantosti, D., 2008. Twenty years of paleoseismology in Italy. Earth-Science Reviews, 88(1-2): 89–117. DOI:http://dx.doi.org/10.1016/j.earscirev.2008.01.001

Giggenbach, W.F., 1992. Isotopic composition of geothermal water and steam discharges. In: D'Amore, F. (Ed.), Application of Geochemistry in Geothermal Reservoir Development. UNITAR/UNDP Centre on Small Energy Resources, Rome, Italy, pp. 253-273.

Giustini, F., Blessing, M., Brilli, M., Lombardi, S., Voltattorni, N., Widory, D., 2013. Determining the origin of carbon dioxide and methane in the gaseous emissions of the San Vittorino plain (Central Italy) by means of stable isotopes and noble gas analysis. Applied Geochemistry, 34: 90-101. DOI:http://dx.doi.org/10.1016/j.apgeochem.2013.02.015

Governa, M.E., Masciocco, L., Riba, M., Zuppi, G.M., Lombardi, S., 1989. Karst and geothermal water circulation in the Central Apennines (Italy), Isotope techniques in the study of the hydrology of fractured and fissured rocks. International Atomic Energy Agency (IAEA), Vienna, pp. 173-202.

King, C.-Y., Koizumi, N., Kitagawa, Y., 1995. Hydrogeochemical anomalies and the 1995 Kobe earthquake. Science, 269(5220): 38–40. DOI:10.1126/science.269.5220.38

Li, X., Liu, W., 2011. Effect of preservation on the $\delta^{13}C$ value of dissolved inorganic carbon in different types of water samples. Isotopes in environmental and health studies, 47(3): 379-389.

Malinverno, A., Ryan, W.B., 1986. Extension in the Tyrrhenian Sea and shortening in the Apennines as result of arc migration driven by sinking of the lithosphere. Tectonics, 5: 227–245. DOI:10.1029/TC005i002p00227

Marini, L., Chiodini, G., Cioni, R., 1986. New geothermometers for carbonateevaporite geothermal reservoirs. Geothermics, 15: 77-86.

Masi, U., Tucci, P., Azzaro, E., 1995. Chemiostratigrafia e petrografia della formazione dolomitica triassica di Antrodoco (Rieti, Lazio settentrionale). Geologica Romana, 31: 307-318.

Formattato: Italiano (Italia)

Formattato: Italiano (Italia)

Codice campo modificato

Formattato: Italiano (Italia)

Codice campo modificato

Formattato: Italiano (Italia)

Formattato: Italiano (Italia)

McSween, H.Y.J., Richardson, S.M., Uhle, M.E., 2003. Geochemistry: Pathways and Processes. Columbia University Press, New York.

Minissale, A.A., Duchi, V., 1988. Geothermometry on fluids circulating in a carbonate reservoir in north-central Italy. Journal of Volcanology and Geothermal Research, 35: 237-252. DOI:https://doi.org/10.1016/0377-0273(88)90020-0

Mongelli, F., Zito, G., 1991. Flusso di calore nella regione Toscana. Studi Geologici Camerti, 1: 91–98. DOI:http://dx.doi.org/10.15165/studgeocam-1177

Mook, W.G., 1976. The dissolution-exchange model for dating groundwater with 14 C. In Interpretation of environmental isotope and hydrochemical data in groundwater hydrology, Advisory group meeting on interpretation of environmental isotope and hydrochemical data in groundwater hydrology. International Atomic Energy Agency (IAEA), Vienna, Austria, pp. 213-225.

Mook, W.G., 1980. Carbon-14 in hydrogeological studies. In: Fritz, P., Fontes, J.-C. (Eds.), Handbook of Environmental Isotope Geochemistry - The Terrestrial Environment A. Elsevier, New York, pp. 49-74.

Onda, S., Sano, Y., Takahata, N., Kagoshima, T., Miyajima, T., Shibata, T., Pinti, D.L., Lan, T., Kim, N.K., Kusakabe, M., Y., N., 2018. Groundwater oxygen isotope anomaly before the M6.6 Tottori earthquake in Southwest Japan. Scientific Reports, 8(1). DOI:https://doi.org/10.1038/s41598-018-23303-8

OriginLab, 2017. Origin User Guide. OriginLab Corporation, Northampton, MA.

Parkhurst, D.L., Appelo, C.A.J., 2013. Description of input and examples for PHREEQC version 3—a computer program for speciation, batch-reaction, one-dimensional transport, and inverse geochemical calculations, (USGS), available only at https://pubs.usgs.gov/tm/06/a43/.

Parkhurst, D.L., Charlton, S.R., 2008. NetpathXL – an Excel Interface to the Program NETPATH - U.S. Geological Survey Techniques and Methods 6–A26, Reston, Virginia.

Person, M., Baumgartner, L., Bos, B., Connolly, J., Gratier, J.P., Gueydan, F., Miller, S.A., Rosenberg, C.L., Urai, J.L., Yardley, B.W.D., 2007. Group report: Fluids, geochemical cycles, and mass transport in fault zones. In: Handy, M.R., Hirth, G., Hovius, N. (Eds.), Tectonic Faults - Agents of Change on a Dynamic Earth. Report of the 95th Dahlem Workshop on The Dynamics of Fault Zones Berlin, January 16–21, 2005. Massachusetts Institute of Technology and Freie Universität Berlin, China, pp. 403-425.

Petitta, M., Fracchiolla, D., Aravena, R., Barbieri, M., 2009. Application of isotopic and geochemical tools for the evaluation of nitrogen cycling in an agricultural basin, the Fucino Plain, Central Italy. Journal of Hydrology, 372: 124–135. DOI:https://doi.org/10.1016/j.jhydrol.2009.04.009

Petitta, M., Primavera, P., Tuccimei, P., Aravena, R., 2011. Interaction between deep and shallow groundwater systems in areas affected by Quaternary tectonics (Central Italy): a geochemical and isotope approach. Environmental Earth Sciences, 63(1): 11-30.

Plummer, N., Prestemon, E.C., Parkhurst, D.L., 1994. An interactive code (NETPATH) for modeling NET geochemical reactions along a flow PATH, version 2.0, U.S. Geological Survey; USGS Earth Science Information Center, Open-File Reports Section.

Ponziani, F., De Franco, R., Minelli, G., Biella, G., Federico, C., Pialli, G., 1995. Crustal shortening and duplication of the Moho in the Northern Apennines: a view from seismic refraction data. Tectonophysics, 252(1-4): 391–418. DOI:https://doi.org/10.1016/0040-1951(95)00093-3

Formattato: Italiano (Italia)

Codice campo modificato

Formattato: Italiano (Italia)

Formattato: Italiano (Italia)

Riguzzi, F., Crespi, M., Devoti, R., Doglioni, C., Pietrantonio, G., Pisani, A.R., 2012. Geodetic strain rate and earthquake size: New clues for seismic hazard studies. Physics of the Earth and Planetary Interiors, 206-207: 67-75. DOI:https://doi.org/10.1016/j.pepi.2012.07.005

Roberts, G.P., Michetti, A., 2004. Spatial and temporal variations in growth rates along active normal fault systems; an example from the Lazzio–Abruzzo Apennines, central Italy. Journal of Structural Geology, 26: 339–376. DOI:https://doi.org/10.1016/S0191-8141(03)00103-2

Romano, M.A., Nardis, R.D., Garbin, M., Peruzza, L., Priolo, E., Lavecchia, G., Romanelli, M., 2013. Temporary seismic monitoring of the Sulmona area (Abruzzo, Italy): A quality study of microearthquake locations. . Natural Hazards and Earth System Sciences, 13(11): 2727-2744. DOI:10.5194/nhess-13-2727-2013

Rosen, M.R., Binda, G., Archer, C., Pozzi, A., Michetti, A.M., Noble, P.J., 2018. Mechanisms of Earthquake-Induced Chemical and Fluid Transport to Carbonate Groundwater Springs After Earthquakes. Water Resources Research, 54(8): 5225-5244. DOI:https://doi.org/10.1029/2017WR022097

Sanjuan, B., Romain, M., Ásmundsson, R., Michel, B., Giroud, N., 2014. Use of two new Na/Li geothermometric relationships for geothermal fluids in volcanic environments. Chemical Geology, 389: 60–81. DOI:http://dx.doi.org/10.1016/j.chemgeo.2014.09.011

Santilano, A., Trumpy, E., Gola, G., Donato, A., Scrocca, D., Ferrarini, F., Brozzetti, F., de Nardis, R., Lavecchia, G., Manzella, A., 2019. A Methodology for Assessing the Favourability of Geopressured-Geothermal Systems in Sedimentary Basin Plays: A Case Study in Abruzzo (Italy). Geofluids. DOI:https://doi.org/10.1155/2019/4503943

Schoeller, H., 1962. Les Eaux Souterraines. Hydrologie dynamique et chimique, Recherche, Exploitation et Évaluation des Ressources. Masson et Cie, Paris.

Scrocca, D., 2006. Thrust front segmentation induced by differential slab retreat in the Apennines. Terra Nova, 18(2): 154–161. DOI: https://doi.org/10.1111/j.1365-3121.2006.00675.x

Sheppard, S.M.F., 1986. Characterization and isotope variations in natural waters. . In: Valley, J.W., Taylor, H.P., O'Neil, J.R. (Eds.), Stable Isotopes in High Temperature Geological Processes. De Gruyter, Berlin/Munich/Boston, pp. 165-184. DOI:https://doi.org/10.1515/9781501508936-011

Siegle, D., 2009. Is there a relationship (difference) or isn't there a relationship (difference)? Neag School of Education – University of Connecticut, https://researchbasics.education.uconn.edu/statistical_significance/#.

Skelton, A., Andrén, M., Kristmannsdóttir, H., Stockmann, G., Mörth, C.M., Sveinbjörnsdóttir, A., Jónsson, S., Sturkell, E., Guðrúnardóttir, H.R., Hjartarson, H., Siegmund, H., Kockum, I., 2014. Changes in groundwater chemistry before two consecutive earthquakes in Iceland. Nature Geoscience, 7: 752–756. DOI:https://doi.org/10.1038/NGEO2250

Skelton, A., Liljedahl-Claesson, L., Wästeby, N., Andrén, M., Stockmann, G., Sturkell, E., Mörth, C.-M., Stefansson, A., Tollefsen, E., Siegmund, H., Keller, N., Kjartansdóttir, R., Hjartarson, H., Kockum, I., 2019. Hydrochemical changes before and after earthquakes based on long term measurements of multiple parameters at 2 sites in northern Iceland–A review. Journal of Geophysical Research: Solid Earth: 2702–2720. DOI:https://doi.org/10.1029/2018JB016757

Smeraglia, L., Bernasconi, S.M., Berra, F., Billi, A., Boschi, C., Caracausi, A., Carminati, E., Castorina, F., Doglioni, C., Italiano, F., Rizzo, A.L., Uysal, T., Zhao, J.-x., 2018. Crustal-scale fluid circulation and co-

Formattato: Italiano (Italia)
Codice campo modificato
Formattato: Italiano (Italia)
Codice campo modificato
Formattato: Italiano (Italia)
Formattato: Italiano (Italia)

seismic shallow comb-veining along the longest normal fault of the central Apennines, Italy. Earth and Planetary Science Letters, 498: 152-168. DOI:https://doi.org/10.1016/j.epsl.2018.06.013

Smeraglia, L., Berra, F., Billi, A., Boschi, C., Carminati, E., Doglioni, C., 2016. Origin and role of fluids involved in the seismic cycle of extensional faults in carbonate rocks. Earth and Planetary Science Letters, 450: 292-305. DOI:https://doi.org/10.1016/j.epsl.2016.06.042

Spötl, C., 2005. A robust and fast method of sampling and analysis of $\delta^{13}C$ of dissolved inorganic carbon in ground waters. Isotopes in Environmental and Health Studies, 4(3): 217-221.

Tassi, F., Cabassi, J., Rouwet, D., Palozzi, R., Marcelli, M., Quartararo, M., Capecchiacci, F., Nocentini, M., Vaselli, O., 2012. Water and dissolved gas geochemistry of the monomictic Paterno sinkhole (central Italy). Journal of Limnology, 71(2): 245-260. DOI:10.4081/jlimnol.2012.e27

Trumpy, E., Manzella, A., 2017. Geothopica and the interactive analysis and visualization of the updated Italian National Geothermal Database. International Journal of Applied Earth Observations and Geoinformation, 54: 28-37. DOI:10.1016/j.jag.2016.09.004

Ünal-İmer, E., Uysal, I.T., Zhao, J.X., Işık, V., Shulmeister, J., Imer, A., Feng, Y.X., 2016. CO_2 outburst events in relation to seismicity: constraints from microscale geochronology, geochemistry of late Quaternary vein carbonates, SW Turkey. Geochimica Cosmochimica Acta, 187: 21–40. DOI:https://doi.org/10.1016/j.gca.2016.05.006

Uysal, I.T., Feng, Y., Zhao, J.X., Isik, V., Nuriel, P., Golding, S.D., 2009. Hydrotermal CO_2 degassing in seismically active zones during the Late Quaternary. Chemical Geology, 265: 442-454. DOI:http://dx.doi.org/10.1016/j.chemgeo.2009.05.011

Vogel, J.C., Grootes, P.M., Mook, W.G., 1970. Isotope fractionation between gaseous and dissolved carbon dioxide. Zeitschrift für Physik A Hadrons and Nuclei, 230(3): 255-258.

Wieser, M.E., 2006. Atomic weights of the elements 2005 (IUPAC Technical Report). Pure and Applied Chemistry, 78(11): 2051-2066.

Williams, R.T., Goodwin, L.B., Sharp, W.D., Mozley, P.S., 2017. Reading a 400,000-year record of earthquake frequency for an intraplate fault. Proceedings of the National Academy of Sciences,, 114: 4893–4898. DOI:https://doi.org/10.1073/pnas.1617945114

Wu, L., Zheng, S., De Santis, A., Qin, K., Di Mauro, R., Liu, S., Rainone, M.L., 2016. Geosphere coupling and hydrothermal anomalies before the 2009 Mw 6.3 L'Aquila earthquake in Italy. Natural Hazards and Earth System Sciences, 16: 1859–1880. DOI:https://doi.org/10.5194/nhess-16-1859-2016

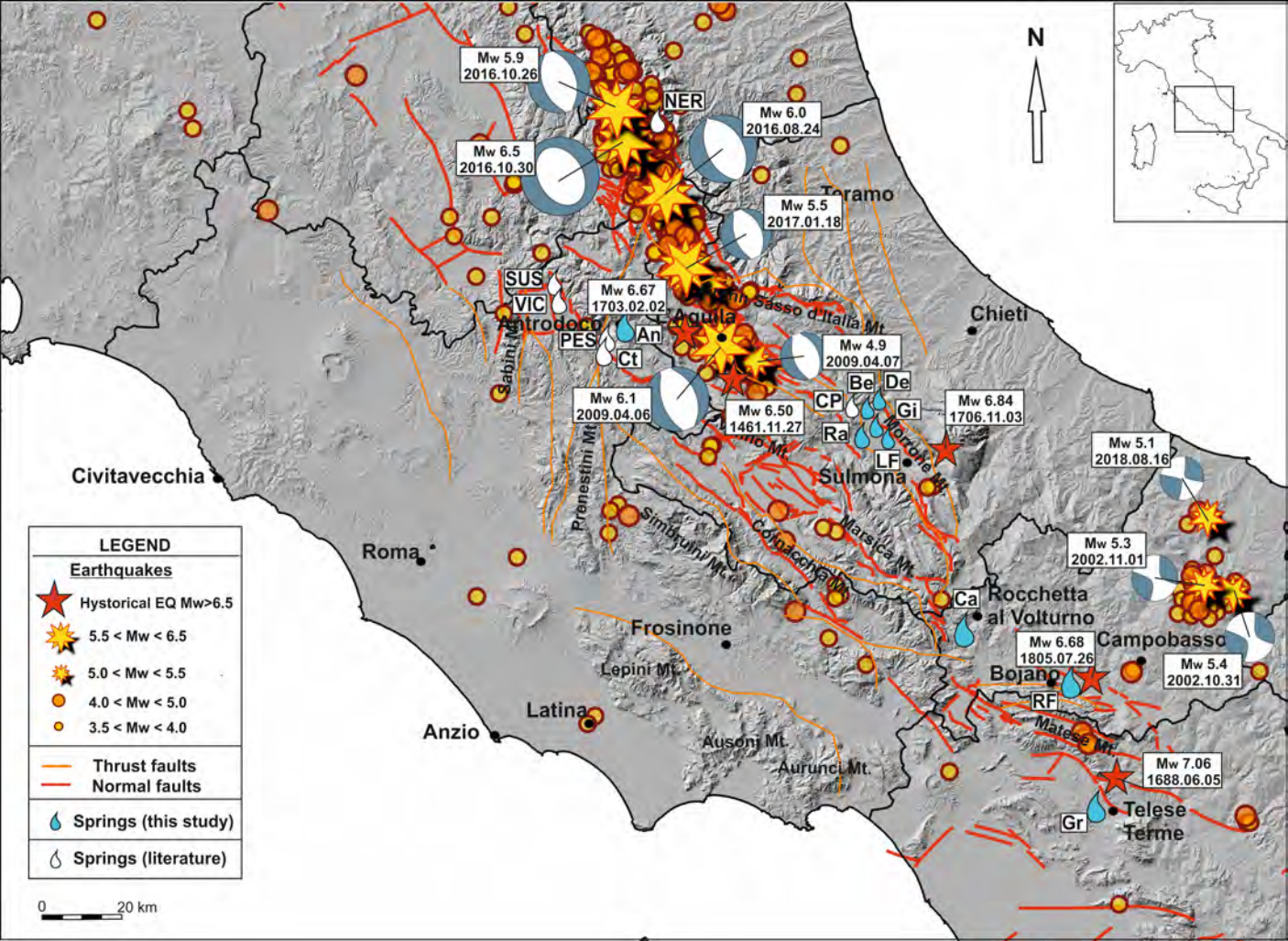
N
Mw 5.9
2016.10.26
NER
Mw 6.0
2016.08.24
Mw 6.5
2016.10.30
Teramo
Mw 5.5
2017.01.18
SUS
VIC
Mw 6.67
1703.02.02
Gran Sasso d'Italia Mt.
Chieti
Antrodoco
PES
An
L'Aquila
Ct
Mw 4.9
2009.04.07
Sabini Mt.
Be
De
CP
Gi
Mw 6.1
2009.04.06
Mw 6.50
1461.11.27
Mw 6.84
1706.11.03
Ra
Morrone Mt.
LF
Mw 5.1
2018.08.16
Civitavecchia
Sulmona
Prenestini Mt.
Simbruini Mt.
Cantalacima Mt.
Marsica Mt.
Roma
Mw 5.3
2002.11.01
Ca
Rocchetta
al Volturno
Frosinone
Mw 6.68
1805.07.26
Campobasso
Lepini Mt.
Bojano
Mw 5.4
2002.10.31
RF
Latina
Matese Mt.
Anzio
Ausoni Mt.
Aurunci Mt.
Mw 7.06
1688.06.05
Gr
Telese
Terme
LEGEND
Earthquakes
Hystorical EQ Mw>6.5
5.5 < Mw < 6.5
5.0 < Mw < 5.5
4.0 < Mw < 5.0
3.5 < Mw < 4.0
Thrust faults
Normal faults
Springs (this study)
Springs (literature)
0
20 km

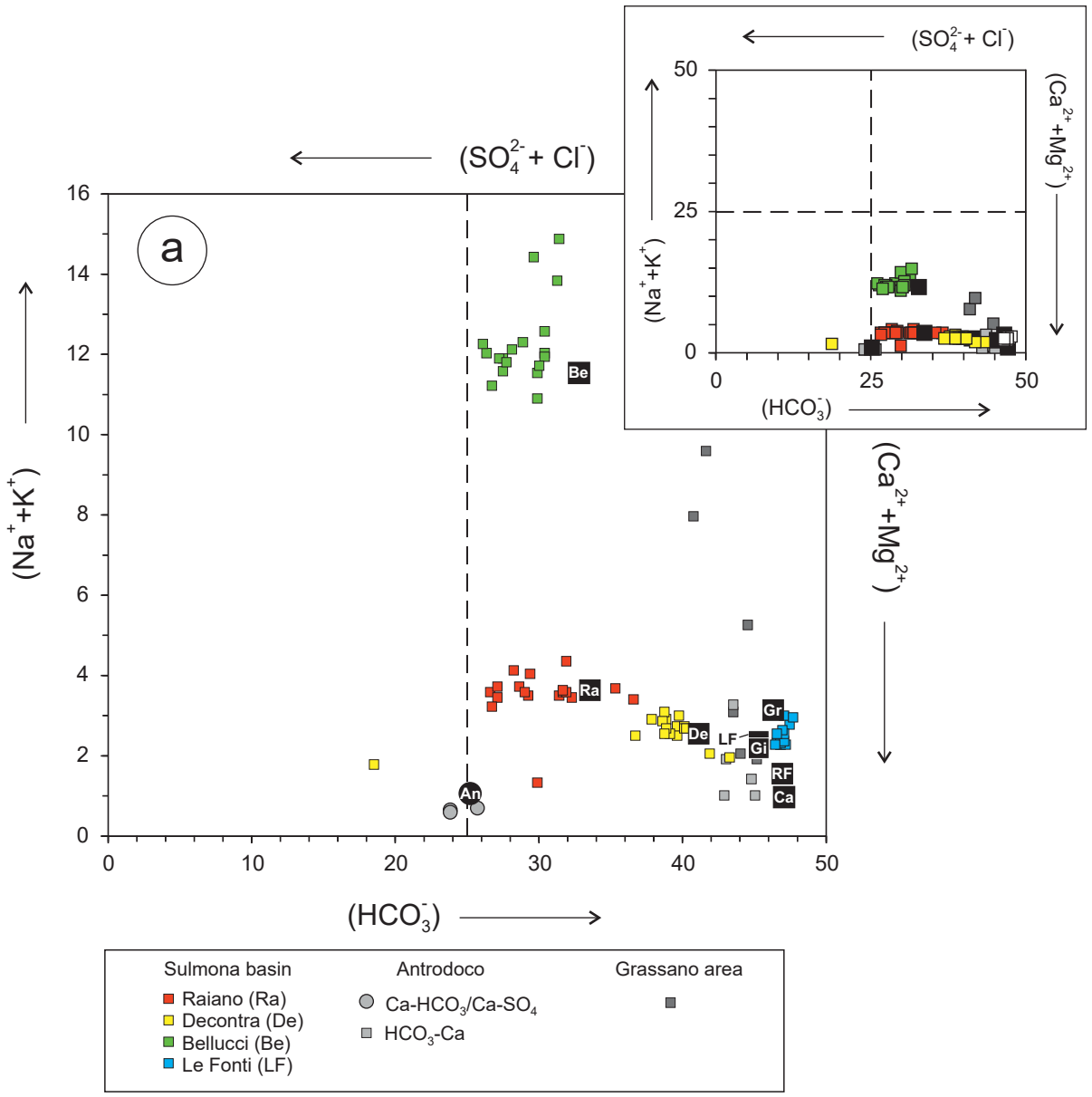
a
$(SO_4^{2-} + Cl^-)$
$(Na^+ + K^+)$
$(Ca^{2+} + Mg^{2+})$
(HCO_3^-)
Be
Ra
De
LF
Gr
Gi
RF
Ca
An
Sulmona basin
Raiano (Ra)
Decontra (De)
Bellucci (Be)
Le Fonti (LF)
Antrodoco
Ca-HCO3/Ca-SO4
HCO3-Ca
Grassano area

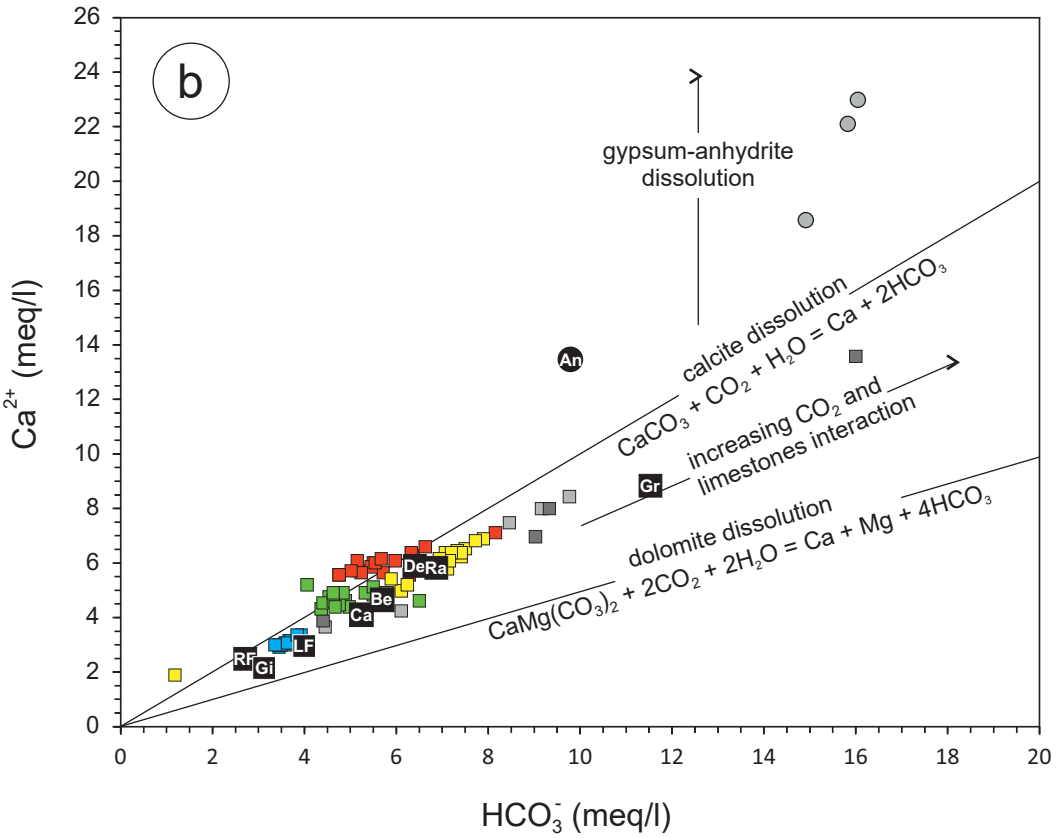
b
Ca^{2+} (meq/l)
HCO_3^- (meq/l)
gypsum-anhydrite dissolution
calcite dissolution
$CaCO_3 + CO_2 + H_2O = Ca + 2HCO_3$
increasing CO_2 and limestones interaction
dolomite dissolution
$CaMg(CO_3)_2 + 2CO_2 + 2H_2O = Ca + Mg + 4HCO_3$
An
Gr
DeRa
Be
Ca
LF
RF
Gi

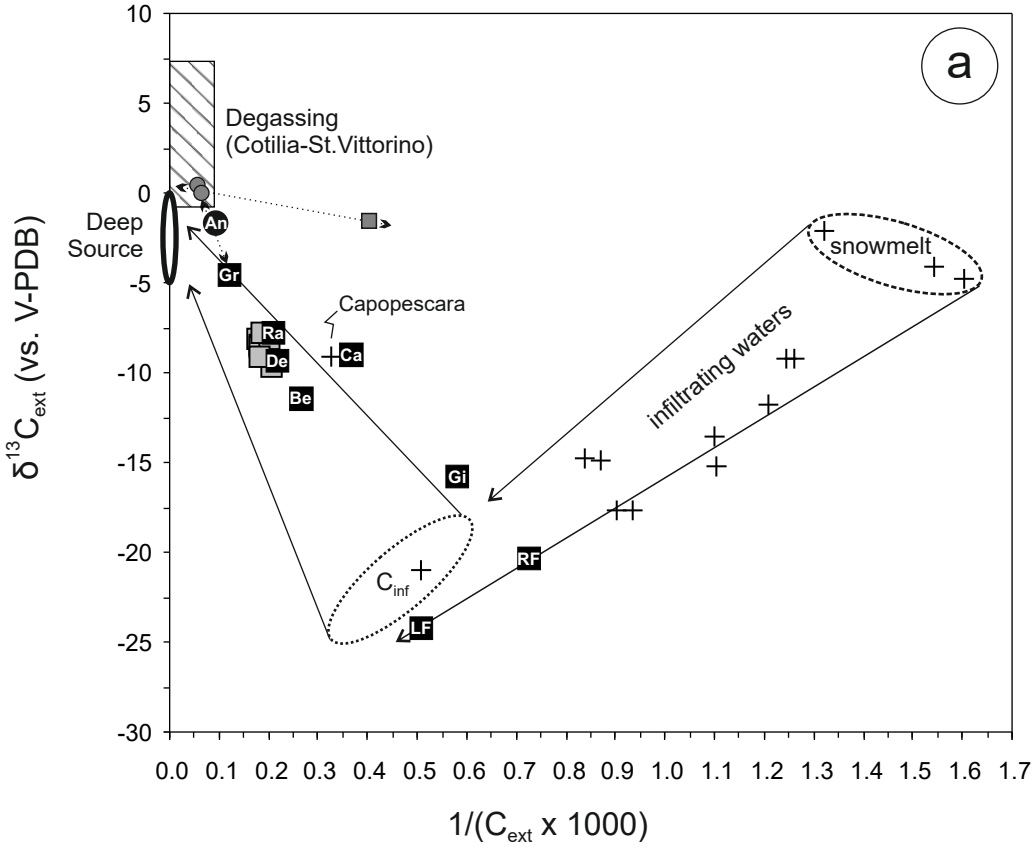
a
Degassing
(Cotilia-St.Vittorino)
Deep
Source
An
Gr
Capopescara
Ra
De
Ca
Be
Gi
RF
LF
C_inf
snowmelt
infiltrating waters
δ13Cext (vs. V-PDB)
1/(Cext x 1000)

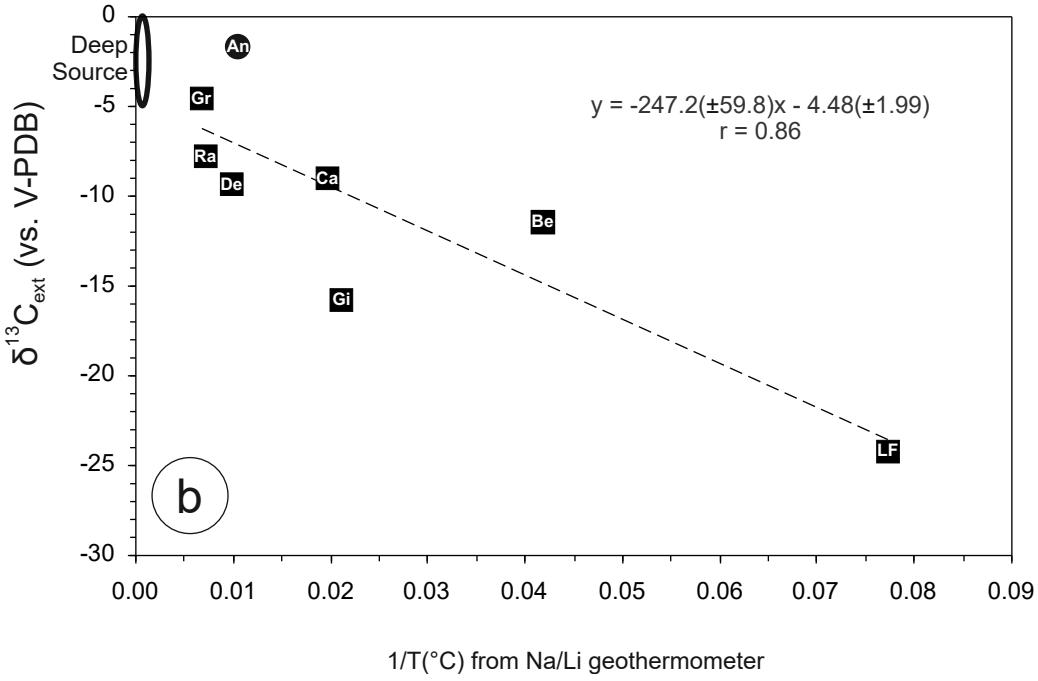
b
Deep
Source
An
Gr
Ra
De
Ca
Be
Gi
LF
y = -247.2(±59.8)x - 4.48(±1.99)
r = 0.86
δ13Cext (vs. V-PDB)
1/T(°C) from Na/Li geothermometer

a) Antrodoco

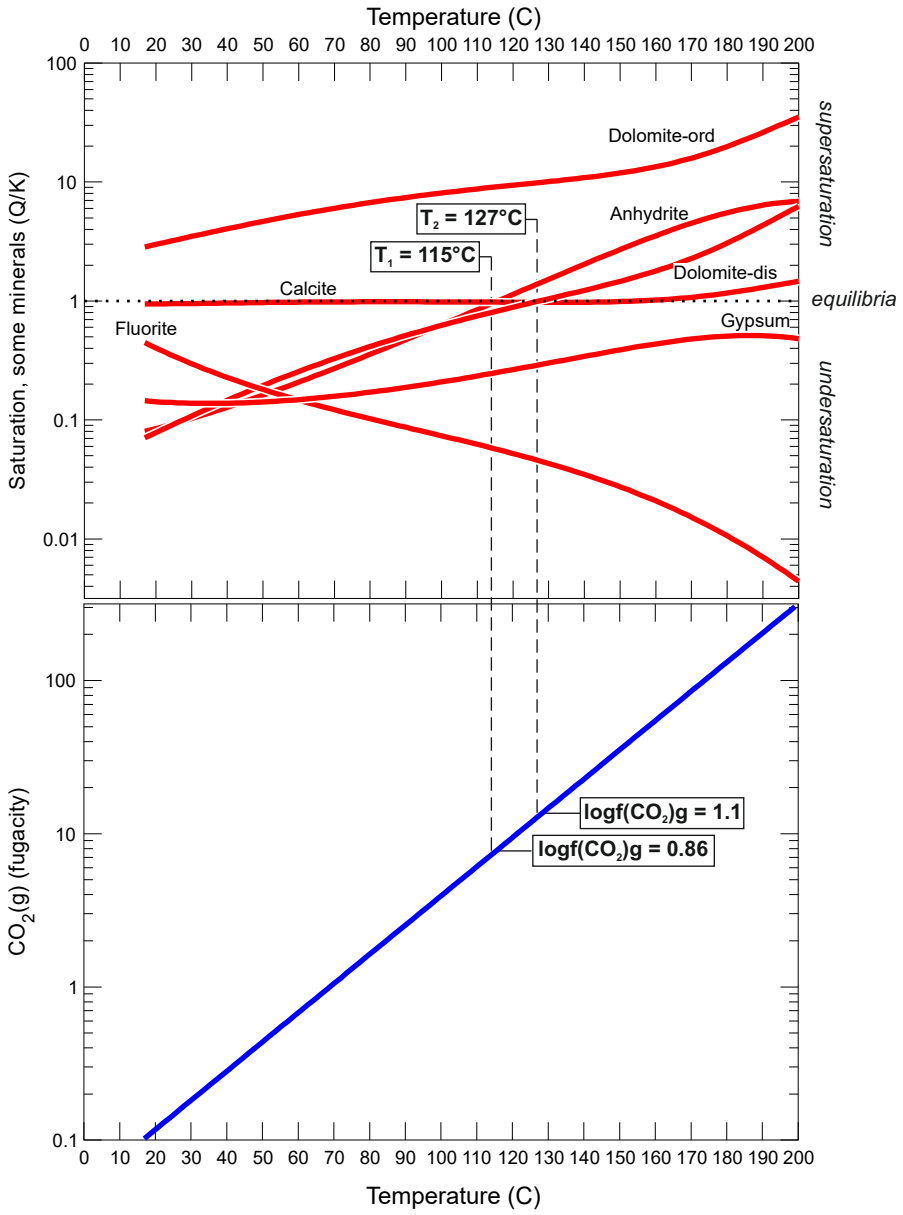

b) Grassano

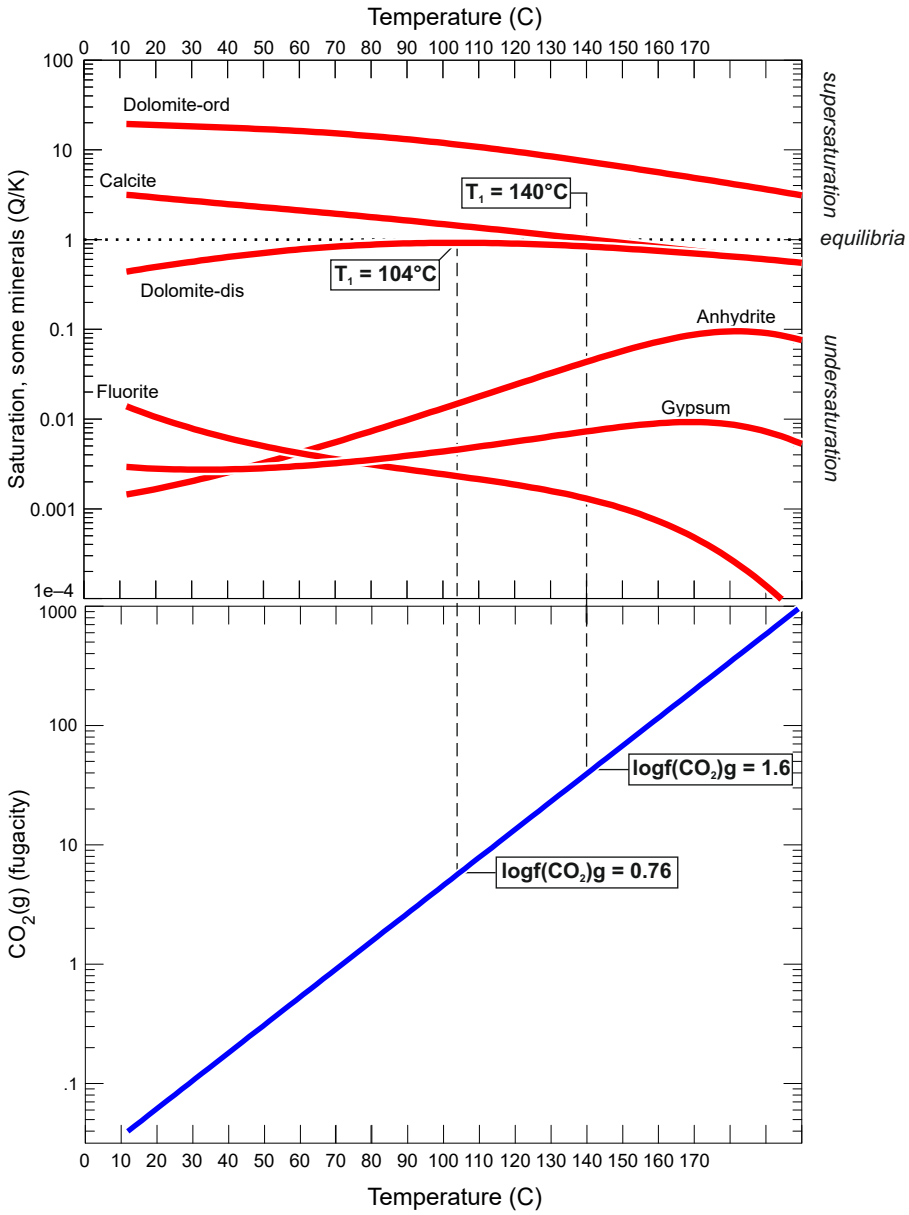

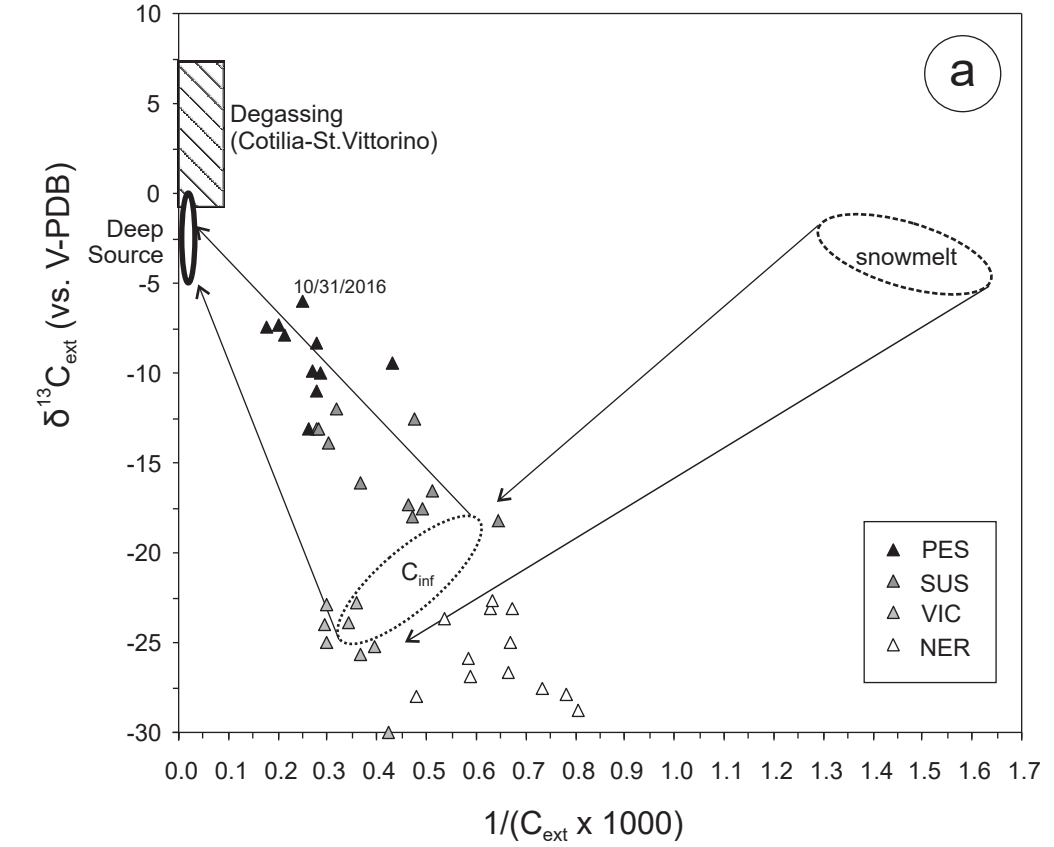
a
Degassing
(Cotilia-St.Vittorino)
Deep
Source
10/31/2016
snowmelt
C_inf
PES
SUS
VIC
NER
δ13Cext (vs. V-PDB)
1/(Cext x 1000)

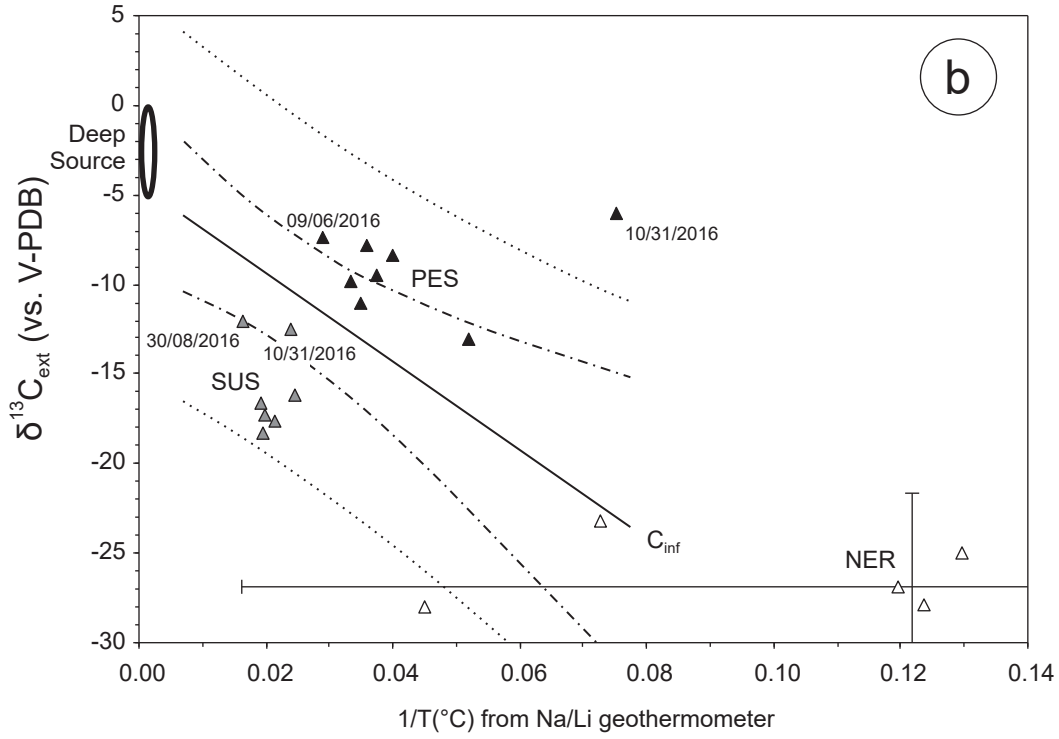
b
Deep
Source
09/06/2016
10/31/2016
PES
30/08/2016
10/31/2016
SUS
C_inf
NER
δ13Cext (vs. V-PDB)
1/T(°C) from Na/Li geothermometer

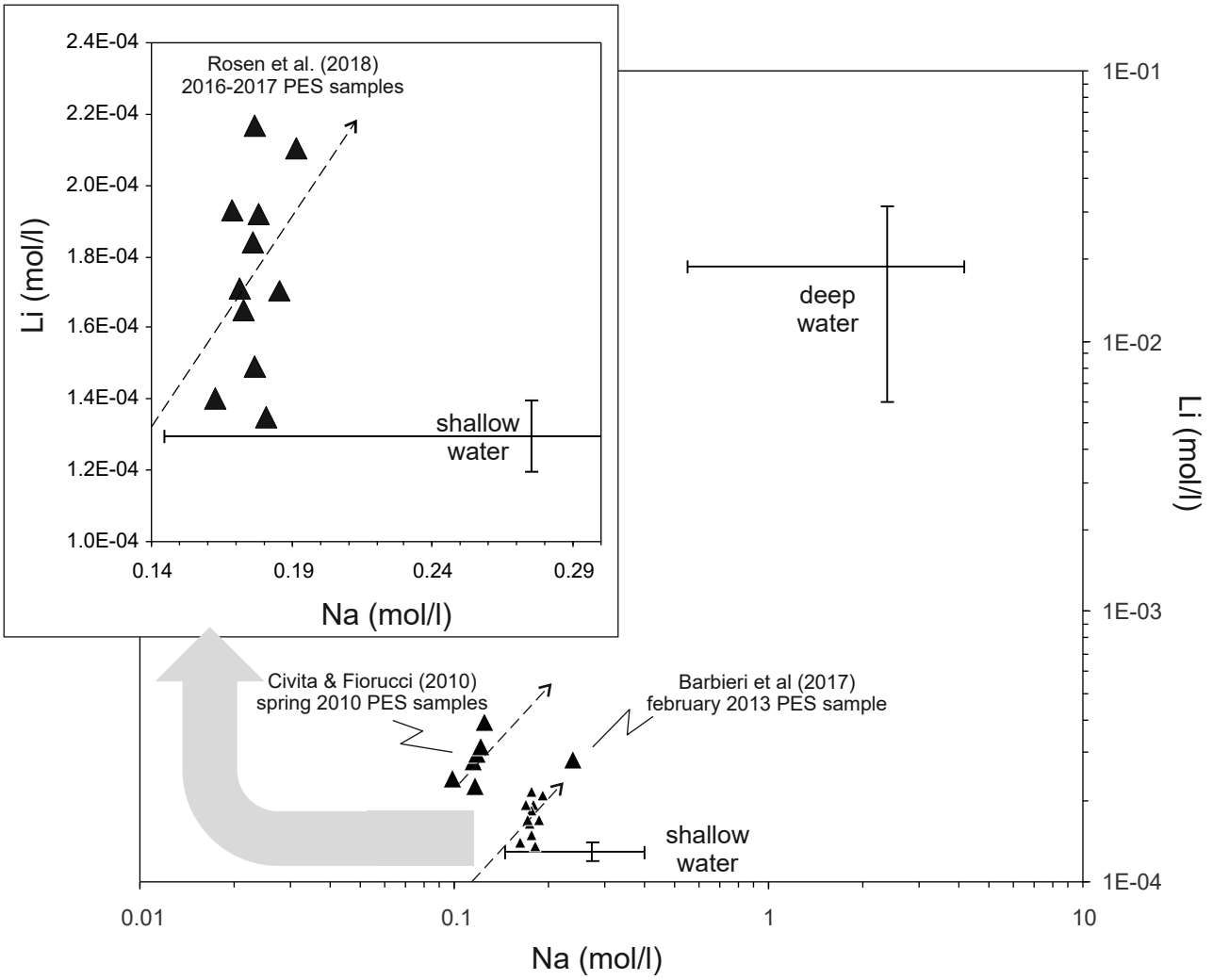
Rosen et al. (2018)
2016-2017 PES samples
Li (mol/l)
2.4E-04
2.2E-04
2.0E-04
1.8E-04
1.6E-04
1.4E-04
1.2E-04
1.0E-04
shallow
water
0.14
0.19
0.24
0.29
Na (mol/l)
deep
water
1E-01
1E-02
1E-03
1E-04
Li (mol/l)
Civita & Fiorucci (2010)
spring 2010 PES samples
Barbieri et al (2017)
february 2013 PES sample
shallow
water
0.01
0.1
1
10
Na (mol/l)

Table 1

sample name	sample code	sampling date	Lat. WGS84	Long. WGS84	elevation m a.s.l.	EC µS/cm	pH -log[H^+]	Temp °C	Ca mg/l	Mg mg/l	Na mg/l	K mg/l	Cl mg/l	SO_4 mg/l	cAlk mg/l	F mg/l	NO_3 mg/l	TDS mg/l	C.I. %	$\delta^{13}C$(DIC) ‰ vs. V-PDB	chemical classification	†thermal classification	T_a local annual air temperature* °C	locality
Le Fonti	LF	5/22/2018	42.118	13.884	313	454	7.614	13.9	60.3	19.7	4.58	1.14	7.97	8.73	243	0.0775	12.8	237	1.8	-10.2	HCO_3-Ca	orthothermal	13.1	Sulmona
Decontra 1	De	5/22/2018	42.178	13.837	249	828	7.103	13.6	119	32.2	13.1	4.05	17.8	127	390	0.291	-	508	-1.5	-4.76	HCO_3-Ca	orthothermal	13.1	Sulmona
Raiano	Ra	5/22/2018	42.108	13.807	285	743	7.071	13.2	118	26.1	8.52	2.30	10.4	57.2	419	0.147	-	432	0.6	-3.66	HCO_3-Ca	orthothermal	13.1	Sulmona
Bellucci	Be	5/22/2018	42.192	13.847	244	758	7.384	13.0	93.6	19.2	41.4	2.99	57.2	64.9	346	0.148	-	452	-3.2	-6.06	HCO_3-Ca	hypothermal	13.1	Sulmona
Giardino	Gi	5/22/2018	42.163	13.841	253	320	7.793	10.0	44.2	11.8	2.94	0.592	4.38	9.55	189	0.0539	1.39	169	-2.1	-7.48	HCO_3-Ca	hypothermal	13.1	Sulmona
Antrodoco	An	5/22/2018	42.421	13.080	493	1642	6.544	16.9	272	67.1	8.17	2.23	9.66	448	488	0.904	8.16	1057	-0.3	-0.477	Ca-HCO_3	orthothermal	12.9	Antrodoco
Capovolturno	Ca	9/7/2018	41.637	14.071	553	494	7.686	11.9	84.4	14.4	1.99	0.629	3.01	11.2	253	0.165	0.849	271	0.8	-3.54	HCO_3-Ca	hypothermal	12.8	Rocchetta a Volturno
Grassano	Gr	9/7/2018	41.225	14.514	55	928	7.075	11.9	179	29.3	15.9	2.33	25.0	9.05	575	0.150	1.89	582	-1.8	-1.84	HCO_3-Ca	hypothermal	13.5	Grassano
Rio Freddo	RF	9/7/2018	41.473	14.497	514	257	7.873	7.9	49.8	5.95	1.89	0.453	4.81	2.10	138	0.363	2.73	152	0.7	-8.70	HCO_3-Ca	hypothermal	12.8	San Polo Matese

E.C. : electrical conductivity

cAlk : carbonate alcalinity as HCO_3

- : not analyzed

TDS : Total Dissolved Solids according to Clescerli (1999)

C.I. : mean charge imbalance calculated by The Geochemist's Workbench®, version 12 (Bethke, 2008), and NetpahXL (Plummer et al., 1994)

* : data from https://it.climate-data.org/info/sources/

† : temperature classification according to Schoeller (1969)

Table 2

sample name	sample code	Na molarity	Li molarity	Na/Li molarity	*Na/Li geotherm. °C	♠ C_{ext} molality	♠ $\delta^{13}C_{ext}$ ‰ vs. V-PDB	♣ $\delta^{13}C_{ext}(CO_2)aq$ ‰ vs. V-PDB	♣ $\delta^{13}C_{ext}(CO_2)g$ ‰ vs. V-PDB	Saturation Indexes and CO_2-gas partial pressure						
										$logPCO_2(g)$	calcite	dolomite-dis	dolomite-ord	anhydrite	gypsum	fluorite
Le Fonti	LF	1.99E-04	1.40E-07	1.43E+03	13	1.97E-03	-24.24	-23.72	-22.62	-2.312	0.23	-0.44	1.19	-3.07	-2.78	-3.2
Decontra 1	De	5.71E-04	3.04E-06	1.88E+02	101	4.58E-03	-9.29	-9.66	-8.55	-1.612	0.13	-0.73	0.90	-1.76	-1.47	-1.9
Raiano	Ra	3.71E-04	3.63E-06	1.02E+02	138	4.82E-03	-7.82	-7.78	-6.67	-1.549	0.14	-0.80	0.84	-2.09	-1.79	-2.5
Bellucci	Be	1.80E-03	1.74E-06	1.04E+03	24	3.76E-03	-11.43	-12.25	-11.13	-1.944	0.27	-0.57	1.07	-2.11	-1.81	-2.5
Giardino	Gi	1.28E-04	2.27E-07	5.64E+02	47	1.73E-03	-15.83	-16.61	-15.49	-2.616	0.14	-0.77	0.89	-3.14	-2.81	-3.7
Antrodoco	An	3.55E-04	1.75E-06	2.03E+02	96	1.07E-02	-1.69	-1.75	-0.649	-0.870	0.04	-0.91	0.70	-1.04	-0.78	-0.8
Capovolturno	Ca	8.67E-05	1.67E-07	5.18E+02	51	2.74E-03	-8.96	-8.76	-7.64	-2.296	0.51	-0.20	1.45	-2.86	-2.55	-2.5
Grassano	Gr	6.90E-04	7.50E-06	9.21E+01	146	8.23E-03	-4.58	-4.66	-3.55	-1.347	0.49	-0.24	1.40	-2.80	-2.49	-2.3
Rio Freddo	RF	8.23E-05	2.49E-08	3.30E+03	-12	1.38E-03	-20.29	-20.06	-18.92	-2.758	0.20	-1.04	0.64	-3.74	-3.39	-1.9

* : from Sanjuan et al. (2014), equation 7 (for chloride concetrations < 0.3M) T°C = {1074/[log(Na/Li)+0.60]} - 273.15

♠ : calculated by Chiodini et al.'s (2000, 2004) method using δC_{carb} = 2.2 ‰ for calcite and dolomite minerals (Fondini et al. 2018; Di Luccio et al. 2018)

♣ : calculated by NetpathXL (Plummer et al. 1994) using δC_{carb} = 2.2 ‰ for calcite and dolomite minerals and activating the "ions charge balance" correction function of the code.

Table 3

sample	ID	mean T	vsp at mean T			total P = 100 MPa		
		°C	pH	$\log PCO_2$	$\delta^{13}C_{ext}(CO_2)g$	pH	$\log PCO_2$	$\delta^{13}C_{ext}(CO_2)g$
Antrodoco	An	113	5.2	1.0	0.130	4.9	1.5	0.226
Grassano	Gr	130	5.5	1.2	-1.28	4.9	1.8	-1.11
Raiano	Ra	128	5.7	0.87	-3.36	5.1	1.3	-3.08

vsp = vapour saturated pressure